

Semi-supervised Community Detection using Glauber Dynamics for an Ising Model

Konstantin Avrachenkov

Inria

Sophia Antipolis, France

k.avrachenkov@inria.fr

Diego Goldsztajn

Universidad ORT Uruguay

Montevideo, Uruguay

goldsztajn@ort.edu.uy

June 10, 2025

Abstract

We consider graphs with two communities and analyze an algorithm for learning the community labels when the edges of the graph and only a small fraction of the labels are known in advance. The algorithm is based on the Glauber dynamics for an Ising model where the energy function includes a quadratic penalty on the magnetization. The analysis focuses on graphs sampled from a Stochastic Block Model (SBM) with slowly growing mean degree. We derive a mean-field limit for the magnetization of each community, which can be used to choose the run-time of the algorithm to obtain a target accuracy level. We further prove that almost exact recovery is achieved in a number of iterations that is quasi-linear in the number of nodes. As a special case, our results provide the first rigorous analysis of the label propagation algorithm in the SBM with slowly diverging mean degree. We complement our theoretical results with several numerical experiments.

Key words: semi-supervised learning, community detection, stochastic block model, Glauber dynamics, Ising model, mean-field limit, almost exact recovery.

Authors are listed alphabetically. Part of this work was done while Diego Goldsztajn was with Inria, the other part was carried out while he was with Universidad ORT Uruguay and was supported by ANII Uruguay under fellowship PD_NAC.2024_182118.

1 Introduction

We consider a Stochastic Block Model (SBM) with two communities in the limiting regime where the mean degree diverges at an arbitrarily slow rate. We assume that labels indicating the communities of a small fraction of nodes are revealed in advance, and consider the semi-supervised learning problem of obtaining the remaining labels using the graph structure. For this purpose, we identify the community labels with positive or negative spins and propose an algorithm based on the Glauber dynamics for the Gibbs probability distribution given by a nonstandard Ising model. In particular, this model is motivated by the maximum likelihood estimator for the true configuration of spins and includes a quadratic penalty on the total magnetization, i.e., the sum of all the spins.

Our algorithm is initialized by assigning the correct spin to the nodes with disclosed community labels, and uniformly random spins to all the other nodes. Then this initial configuration of spins evolves as the continuous-time Markov chain given by the Glauber dynamics for our Ising model. Specifically, each spin flips independently from the other spins at a rate that depends on how it compares to the neighboring spins and the quadratic penalty. We characterize the amount of time that the Glauber dynamics must evolve for the classification error to be below a target threshold, and establish that almost exact recovery is achieved after a number of spin flips that is quasi-linear in the number of nodes.

1.1 Overview of main results

Let n be the number of nodes and suppose that the average degree scales as λ_n . Our algorithm includes two hyperparameters: α_n is the weight assigned to the quadratic penalty and β_n is the inverse temperature associated with the Gibbs probability distribution. We assume that $\lambda_n \rightarrow \infty$ and $\beta_n \lambda_n \rightarrow \infty$ as $n \rightarrow \infty$, and show that our algorithm is effective if α_n is in a range of values given by the connectivity parameters of the SBM, which can be estimated using the revealed labels. Specifically, we obtain the following results.

1. *Mean-field limit.* We establish that the vector-valued process which describes the magnetization of each community converges weakly to the solution of a differential equation. Since the classification error can be expressed in terms of this vector, the differential equation can be used to decide the simulation time t_{end} for the Glauber dynamics, so that the classification error is below a given threshold. Given the target error and the simulation time, our algorithm involves $O(nt_{\text{end}})$ spin flips. To the best of our knowledge, we are the first to characterize the effort needed by a graph clustering algorithm to achieve a target level of accuracy.
2. *Almost exact recovery.* We show that a vanishing fraction of incorrect community labels is obtained if the simulation time diverges slowly with n instead of remaining constant as above. In this case, our algorithm involves $O(n \log \lambda_n)$ spin flips.

3. *Analysis of Label Propagation.* The above results cover the special case when $\alpha_n = 0$ and $\beta_n = \infty$ for all n , which corresponds to the Label Propagation or Majority Vote algorithm proposed for clustering problems in [39]. The interdependence of nonlinear dynamics and graph topology creates significant challenges for the analysis on random graphs. To the best of our knowledge, we are the first to rigorously analyze this algorithm in the SBM with a slowly diverging mean degree.
4. *Numerical results.* The range of admissible values for α_n is an interval that typically contains zero; the more symmetric the community sizes are, the larger this interval is. While our asymptotic results hold as long as α_n lies in this interval, we observe numerically that our algorithm performs better when the quadratic penalty is active with $\alpha_n > 0$; we explain this intuitively relying on some of our proof arguments. We also observe numerically that our algorithm performs better than several other semi-supervised community detection algorithms with comparable complexity.

Mean-field limits are unusual in the clustering literature, but as observed above, have the advantage of characterizing how the classification error evolves over time, which can be leveraged to estimate the time required by the algorithm to achieve a target accuracy level. Standard mean-field arguments can be used to describe the macroscopic behavior of particles interacting in a way that makes them statistically exchangeable; see the pioneering papers [6, 29–31]. In contrast, the spins that we consider are not exchangeable because the flip rate of a spin depends on the graph neighborhood, which varies across the spins. A further challenge is that the random graph and the current configuration of spins are not independent, because the flip rates of spins depend on the graph structure. In addition, the flip rates depend on the sums of neighboring spins in a way that becomes discontinuous in the limit as $n \rightarrow \infty$, which complicates the analysis even further.

Our proofs use concentration inequalities to approximate the sums of neighboring spins by quantities that depend on the magnetizations of the communities and the connectivity parameters of the graph. We prove that these approximations become exact in the limit, and allow to describe the evolution of the magnetization vector through a differential equation. The almost exact recovery result does not follow from the mean-field limit, which concerns process-level convergence over finite intervals of time, and requires additional arguments for analyzing the Glauber dynamics over a diverging time horizon.

1.2 Related work

Graph clustering or community detection is a central problem in machine learning with many applications, e.g., social [7, 22, 48] and biological [8, 11] networks, bibliometrics [14, 45] and image processing [43, 46]. Many theoretical and practical aspects of this problem have been comprehensively discussed in several surveys and books; see [3, 20, 34, 37, 42].

The SBM considered in this paper is an inhomogeneous Erdős-Rényi random graph model, which is a simple but fundamental model for communities in a graph that has been extensively used in the context of clustering. This model is usually analyzed in limiting regimes where the number of nodes goes to infinity, and clustering problems are classified in terms of the fraction of incorrect community labels considered admissible. In this paper we focus on partial and almost exact recovery problems. The former require that a given (and typically large) fraction of labels are correctly identified with probability tending to one, and the latter that all but a vanishing fraction of labels are correct. Other objectives are exact recovery, which corresponds to correctly identifying all the labels with high probability, and weak recovery, which only requires that the learned labels are positively correlated with the true labels and is most relevant in the constant-degree regime.

Many papers have considered the above clustering problems in the unsupervised case where no labels are disclosed in advance. For this situation we refer to the foundational works [2, 10, 35], and the survey [1], where the information-theoretic limits and efficient algorithms for unsupervised clustering in the SBM are extensively discussed.

1.2.1 Graph-based semi-supervised learning

Unlike the literature surveyed in [1], we assume that a small fraction of community labels are revealed in advance, which is called semi-supervised learning in the machine learning community. This situation is prevalent in practice and can significantly improve the efficacy and efficiency of graph clustering, as observed in [13, 44, 47, 50, 51].

In the context of the SBM, information-theoretic limits for exact recovery with side information and logarithmic mean degree are derived in [41], which further proposes a clustering algorithm based on eigenelements. Another semi-supervised algorithm, based on a constrained linear system, is defined in [4] and is shown to achieve almost exact recovery if the mean degree diverges at any rate. Both algorithms have polynomial complexity in the number of nodes; significantly larger than our quasi-linear algorithm. Recently, [49] showed that almost exact recovery in the SBM is achieved by a gossiping algorithm in quasi-linear time. However, in [49] the average degree is super-logarithmic in the number of nodes, and the density of intra-cluster edges grows faster than that of inter-cluster edges, making the setup substantially less challenging than in this paper.

A class of semi-supervised consensus and label propagation algorithms converge in quasi-linear time and have shown remarkable efficacy on both synthetic and real-world data [21, 39, 50, 51]; however, their classification error has not been rigorously characterized to the best of our knowledge. Since our algorithm also has quasi-linear time complexity, our numerical study compares our algorithm against the latter class. Specifically, we consider consensus-based algorithms [51], generalized Laplacian-based algorithms [5, 50] (including PageRank based algorithm) and the Poisson Learning algorithm [12]. Our numerical results show that our algorithm achieves a much smaller classification error than all these

algorithms, and in addition needs to perform considerably fewer updates per node.

1.2.2 Ising models on random graphs

Using Ising models and Glauber dynamics for graph clustering has been proposed and empirically evaluated for unsupervised problems in [40]. In particular, it was observed that the energy function with the penalty on magnetization corresponds to the modularity of the network (as defined in [38]) with the Erdős-Rényi graph as a null model. More recently, [32] has proposed similar Glauber dynamics to achieve weak recovery in the constant-degree symmetric SBM. In [32] the information-theoretic limit is not reached and the run-time is roughly of order n^4 in the number of nodes, ignoring polylogarithmic factors; the authors write that this estimate seems conservative and that a quasi-linear time in n should be sufficient for weak recovery. Thus, algorithms based on Glauber dynamics for Ising models are also of interest in the contexts of unsupervised learning and weak recovery, making them widely applicable for various graph clustering tasks.

The Glauber dynamics for the standard Ising model at zero temperature correspond to the majority vote or label propagation algorithm; as noted earlier, this is the same as setting $\alpha_n = 0$ and $\beta_n = \infty$ in our model. Since the initial proposal to apply the label propagation algorithm to clustering in [39], many variations have been proposed and tested on synthetic and real-world data; see, e.g., [24]. Nevertheless, we are not aware of rigorous analytical results besides those in [28] showing that exact recovery is achieved in two rounds of the algorithm under suitable connectivity conditions in the SBM. In particular, in [28] the intra-cluster mean degree grows faster than $n^{3/4}$ and the inter-cluster mean degree grows slower than $n^{1/2}$. We remark that the regime considered in the present paper is significantly more challenging, since the intra and inter-cluster mean degree are of the same order and approach infinity arbitrarily slow. A sampling version of the label propagation algorithm, where updates are based on two random neighbors, has been rigorously analyzed in [15] for the SBM. There, the intra-cluster mean degree must grow faster than $n^{1/2}$ and the cut is quite sparse, which makes the regime less challenging than that considered here.

The series of papers [17–19, 25] studies metastability of the Glauber dynamics for the standard Ising model on various random graph models. However, there are at least three important differences with the present paper. Firstly, the Ising model in the former papers is purely ferromagnetic, whereas we analyze a more complicated model with ferromagnetic as well as antiferromagnetic interactions. Secondly, [17–19, 25] do not study clustered models such as the SBM. Lastly, the latter papers study the asymptotics of the mean crossover time from one metastable state to another, whereas we characterize the transient trajectory towards a set of states with good properties for identifying clusters.

Finally, we observe that several papers [16, 33, 36] have obtained conditions for rapid mixing and cutoff for the Ising model on random graphs, but these phenomena can only appear at sufficiently small inverse temperatures. Furthermore, as noted above, our results

are based on the transient behavior of the Glauber dynamics prior to mixing. We feel that this different approach can present significant interest to researchers working in the areas of statistical physics and interacting particle systems.

1.3 Standard notation

We use the symbols P and E to denote the probability of events and the expectation of functions, respectively. The underlying probability measure to which these symbols refer is always clear from the context or explicitly indicated. For random variables in a common metric space S , we denote the weak convergence of $\{X_n : n \geq 1\}$ to X by $X_n \Rightarrow X$. If the limiting random variable X is deterministic, then this is equivalent to convergence in probability. The left and right limits of a function $f : [0, \infty) \rightarrow S$ are denoted by

$$f(t^-) := \lim_{s \rightarrow t^-} f(s) \quad \text{for all } t > 0 \quad \text{and} \quad f(t^+) := \lim_{s \rightarrow t^+} f(s) \quad \text{for all } t \geq 0,$$

respectively. We say that the function f is càdlàg if the left limits exist for all $t > 0$ and the right limits exist for all $t \geq 0$ and satisfy that $f(t^+) = f(t)$.

1.4 Organization of the paper

The rest of the paper is organized as follows. In Section 2 we give precise descriptions of the semi-supervised community detection problem and our algorithm. In Section 3 we state our main results: a mean-field limit for the magnetization of each community and the almost exact recovery result. These results are proved in Sections 5 and 6, respectively. In Section 7 we prove several key results used to establish the main results. We present and discuss several numerical experiments in Section 8 and conclude the paper in Section 9. The proofs of some intermediate results are deferred until Appendices A and C.

2 Problem formulation

We consider a sequence of simple and undirected graphs $\mathcal{G}_n = (\mathcal{V}_n, \mathcal{E}_n)$. For each graph, the set of nodes $\mathcal{V}_n = \mathcal{V}_n^1 \cup \mathcal{V}_n^2$ is split into two disjoint communities with sizes $V_n^k := |\mathcal{V}_n^k|$. In this paper we use the terms *community* and *cluster* interchangeably. We emphasize that n is just a scaling parameter and $V_n := |\mathcal{V}_n| = V_n^1 + V_n^2$ is the total number of nodes, which scales linearly with n . More specifically, we assume that

$$v^k := \lim_{n \rightarrow \infty} \frac{V_n^k}{n} \in (0, \infty) \quad \text{for all } k \in \{1, 2\}.$$

Each graph \mathcal{G}_n is sampled from a stochastic block model where the intra-community and inter-community edge probabilities are given by

$$a_n := \frac{a\lambda_n}{n} \quad \text{and} \quad b_n := \frac{b\lambda_n}{n},$$

respectively, where $\lambda_n \rightarrow \infty$ as $n \rightarrow \infty$ and $a > b > 0$ are constants. Specifically, if $u \in \mathcal{V}_n^k$ and $v \in \mathcal{V}_n^l$ are two nodes, then the probability that they are connected by an edge is

$$p_n(k, l) := \begin{cases} a_n & \text{if } k = l, \\ b_n & \text{if } k \neq l. \end{cases}$$

Suppose that we do not know in which community each node is except for a small fraction of the nodes. Our objective is to learn almost all the community labels from the small fraction of labels that are known in advance and the edges of the graph.

2.1 Maximum likelihood estimator and Ising model

A configuration or labeling $\sigma : \mathcal{V}_n \rightarrow \{-1, 1\}$ is a mapping that assigns a community label to each node. We denote the space of all configurations on \mathcal{G}_n by Σ_n and use the term *spin*, from the interacting particle systems literature, instead of *community label*. Our approach is motivated by the next standard result, which is proved in Appendix C and provides an expression for the maximum likelihood estimator of the true configuration.

Proposition 1. *Let us define $p_{\mathcal{G}}(\sigma) := P(\mathcal{G}_n = \mathcal{G} \mid \mathcal{V}_n^1 = \sigma^{-1}(1) \text{ and } \mathcal{V}_n^2 = \sigma^{-1}(-1))$ for each graph $\mathcal{G} = (\mathcal{V}_n, \mathcal{E})$ and configuration $\sigma \in \Sigma_n$. Then the maximum likelihood estimator can be expressed as a solution of the following optimization problem:*

$$\operatorname{argmax}_{\sigma \in \Sigma_n} p_{\mathcal{G}}(\sigma) = \operatorname{argmin}_{\sigma \in \Sigma_n} \left\{ -\frac{1}{2} \sum_{u \sim v} \sigma(u)\sigma(v) + \frac{\rho_n}{2} \left[\sum_{u \in \mathcal{V}_n} \sigma(u) \right]^2 \right\}, \quad (1)$$

where $\rho_n := [\log(1 - a_n) - \log(1 - b_n)] / [\log(b_n(1 - a_n)) - \log(a_n(1 - b_n))]$ and $u \sim v$ indicates that the nodes are connected by an edge in the graph \mathcal{G} .

As above, we write $u \sim v$ if u and v are connected by an edge in \mathcal{G}_n , i.e., if $\{u, v\} \in \mathcal{E}_n$. Given some $\alpha \in \mathbb{R}$, we let $\alpha_n := \alpha\lambda_n/n$ and define an energy function $H_n : \Sigma_n \rightarrow \mathbb{R}$ by

$$H_n(\sigma) := -\frac{1}{2} \sum_{u \sim v} \sigma(u)\sigma(v) + \frac{\alpha_n}{2} \left[\sum_{u \in \mathcal{V}_n} \sigma(u) \right]^2 \quad \text{for all } \sigma \in \Sigma_n.$$

This expression coincides with the objective of (1) when $\alpha_n = \rho_n$. However, we let α be a hyperparameter since ρ_n is difficult to estimate exactly. Another hyperparameter of our algorithm is the so-called inverse temperature $\beta_n > 0$. Together with the energy function,

β_n defines a Gibbs probability measure on the space of configurations Σ_n . More specifically, the probability of configuration σ with respect to this measure is

$$\left[\sum_{\rho \in \Sigma_n} e^{-\beta_n H_n(\rho)} \right]^{-1} e^{-\beta_n H_n(\sigma)}. \quad (2)$$

Our energy H_n and the above Gibbs probability measure are closely related to the standard Ising model from statistical mechanics and the generalized modularity [40]. In particular, the first term of H_n appears in the standard energy function for the Ising model; but this energy does not include a quadratic term in the sum of the spins. The first term of H_n tends to be smaller when neighboring nodes have the same spin and is minimal if all the spins have the same sign. However, it is also relatively small for the configurations where the spin is constant within each community and opposite across the communities, since the edge density is higher within the communities. If $\alpha > 0$, then the second term of H_n penalizes the configurations where the sum of the spins is far from zero, and in particular the configurations where the spin is constant over the entire graph.

2.2 Glauber dynamics

Suppose that the spin of $u \in \mathcal{V}_n$ flips and let $\sigma(u)$ denote the spin of u before the change occurs. As a result of this flip, the energy of configuration $\sigma \in \Sigma_n$ changes by

$$\begin{aligned} & -\frac{1}{2} \sum_{\substack{v \sim w \\ v, w \neq u}} \sigma(v)\sigma(w) + \sum_{v \sim u} \sigma(u)\sigma(v) + \frac{\alpha_n}{2} \left[V_n + 2 \sum_{\substack{v < w \\ v, w \neq u}} \sigma(v)\sigma(w) - 2 \sum_{v \neq u} \sigma(u)\sigma(v) \right] \\ & + \frac{1}{2} \sum_{\substack{v \sim w \\ v, w \neq u}} \sigma(v)\sigma(w) + \sum_{v \sim u} \sigma(u)\sigma(v) - \frac{\alpha_n}{2} \left[V_n + 2 \sum_{\substack{v < w \\ v, w \neq u}} \sigma(v)\sigma(w) + 2 \sum_{v \neq u} \sigma(u)\sigma(v) \right]. \end{aligned}$$

The first line is the energy after the spin flips, whereas the second line gives the opposite of the energy before the flip. Thus, the change in the energy is:

$$\Delta_n(\sigma, u) = 2\sigma(u) \left[\sum_{v \sim u} \sigma(v) - \alpha_n \sum_{v \neq u} \sigma(v) \right]. \quad (3)$$

The continuous-time Glauber dynamics are the Markov chain $\{\sigma_n(t) : t \geq 0\}$ on the space of configurations Σ_n such that the spin of each node u flips independently at rate

$$r(\beta_n \Delta_n(\sigma_n, u)) \quad \text{with} \quad r(x) := \frac{1}{1 + e^x} \quad \text{for all } x \in \mathbb{R};$$

throughout the paper we use boldface notation for quantities that evolve over time. In other words, a transition between two configurations $\sigma, \rho \in \Sigma_n$ may occur only if the two

configurations differ exactly at one node. In that case a transition from σ to ρ happens at rate $r(\beta_n(H_n(\rho) - H_n(\sigma)))$. It is not difficult to check that the Markov chain defined in this way is reversible and ergodic with stationary distribution (2).

Remark 1. A discrete-time version of the Glauber dynamics can also be considered. In this version a node $u \in \mathcal{V}_n$ is selected uniformly at random at each time t , and then the spin of this node flips with probability $r(\beta_n \Delta_n(\sigma_n(t), u))$. The two versions of the dynamics are closely related. Indeed, suppose that the configuration at time t is given. Then the configuration reached after a spin flip has the same distribution under both versions of the dynamics. Moreover, let τ_n be the duration of a time slot in the discrete-time version. Then it is not difficult to check that the mean amount of time until a spin flip is

$$\tau_n V_n \left[\sum_{u \in \mathcal{V}_n} r(\beta_n \Delta_n(\sigma_n(t), u)) \right]^{-1} \quad \text{and} \quad \left[\sum_{u \in \mathcal{V}_n} r(\beta_n \Delta_n(\sigma_n(t), u)) \right]^{-1},$$

for the discrete-time and the continuous-time versions, respectively.

We also consider the situation when $\beta_n = \infty$ under the following convention:

$$r(\beta_n x) := \mathbb{1}_{\{x < 0\}} + \frac{1}{2} \mathbb{1}_{\{x = 0\}} \quad \text{for all } x \in \mathbb{R} \quad \text{if } \beta_n = \infty. \quad (4)$$

In this case the spin of $u \in \mathcal{V}_n$ cannot flip when $\Delta_n(\sigma_n, u) > 0$. However, the spin flips at rate 1/2 if this does not change the energy and at unit rate when this reduces the energy. This corresponds to the Label Propagation or Majority Vote algorithm in [39] when $\alpha = 0$, i.e., nodes change their spin to the value that is most popular among their neighbors.

2.3 Semi-supervised learning algorithm

Algorithm 1 outlines our semi-supervised method for learning the community labels when a fraction of them are revealed in advance. The inputs of the algorithm are the fraction of revealed labels η and the simulation time t_{end} for the Glauber dynamics. The latter can be selected as $t_{\text{end}} = \log[2(1 - \eta)/\varepsilon]$ if the relative classification error should be lower than ε . This choice will be justified using our mean-field limit, as we explain in Section 3. Without any loss of generality, the correct labeling corresponds to nodes in community \mathcal{V}_n^1 having positive spin and nodes in community \mathcal{V}_n^2 have negative spin.

If $\alpha = 0$ and nodes have access to the spins of their neighbors, then Algorithm 1 can be implemented in an entirely distributed manner. Otherwise, we need a common variable for the value of the magnetization, which must be updated after each spin flip.

Informally speaking, the Glauber dynamics simulated in Algorithm 1 modify the spins of the nodes in a way that tends to reduce the energy H_n , and the configuration where the spins are positive in \mathcal{V}_n^1 and negative in \mathcal{V}_n^2 can be regarded as a local minimum of H_n . In

Algorithm 1: Semi-supervised algorithm for learning the community labels.

Input: fraction $\eta \in (0, 1]$ of revealed labels and total simulation time $t_{\text{end}} \geq 0$
Parameters: hyperparameter $\alpha_n \in \mathbb{R}$ and inverse temperature $\beta_n > 0$

```

1 for  $u \in \mathcal{V}_n$  do
2   sample  $u$  with probability  $\eta$ ;
3   if sampled then
4     obtain community label from oracle and set  $\sigma_n(0, u) = \mathbb{1}_{\{u \in \mathcal{V}_n^1\}} - \mathbb{1}_{\{u \in \mathcal{V}_n^2\}}$ ;
5   else
6     let  $\sigma_n(0, u)$  be uniformly random in  $\{-1, 1\}$ ;
7 while  $t < t_{\text{end}}$  do
8   simulate the Glauber dynamics  $\sigma_n$  given by (3) (revealed spins may change);
Output: community labels given by  $\sigma_n(t_{\text{end}})$ 

```

Section 3 we will establish that the Glauber dynamics drive the initial configuration $\sigma_n(0)$ constructed in the first steps of the algorithm towards the latter local minimum, provided that the graph is sufficiently large and α is selected suitably.

3 Main results

Before stating the main results, we define some notation that will be used in the rest of the paper. We denote the neighborhood of $u \in \mathcal{V}_n$ and its intersection with \mathcal{V}_n^k by

$$\mathcal{N}_n(u) := \{v \in \mathcal{V}_n : v \sim u\} \quad \text{and} \quad \mathcal{N}_n^k(u) := \{v \in \mathcal{V}_n^k : v \sim u\},$$

respectively, and let $N_n(u) := |\mathcal{N}_n(u)|$ and $N_n^k(u) := |\mathcal{N}_n^k(u)|$. Further, we define

$$\mathcal{Y}_s^k(\sigma) := \{v \in \mathcal{V}_n^k : \sigma(v) = s\} \quad \text{and} \quad \hat{\mathcal{Y}}_s^k(\sigma, u) := \{v \in \mathcal{Y}_s^k(\sigma) : v \sim u\}$$

for all $s \in \{-, +\}$ and $\sigma \in \Sigma_n$, and let $Y_s^k(\sigma) := |\mathcal{Y}_s^k(\sigma)|$ and $\hat{Y}_s^k(\sigma, u) := |\hat{\mathcal{Y}}_s^k(\sigma, u)|$. In addition, the (normalized) magnetization of \mathcal{V}_n^k under configuration $\sigma \in \Sigma_n$ is defined as

$$z^k(\sigma) := \frac{1}{V_n^k} \sum_{u \in \mathcal{V}_n^k} \sigma(u) = \frac{Y_+^k(\sigma) - Y_-^k(\sigma)}{V_n^k} \in [-1, 1] \quad \text{and} \quad \mathbf{z}_n^k(t) := z^k(\sigma_n(t)).$$

The vector-valued magnetization process \mathbf{z}_n has sample paths in the space $D_{\mathbb{R}^2}[0, \infty)$ of càdlàg functions from $[0, \infty)$ into \mathbb{R}^2 , which we endow with the topology of uniform convergence over compact sets. The following mean-field limit is proved in Section 5.

Theorem 1. *Suppose that σ_n evolves as in Algorithm 1 and assume that:*

$$v^1 \geq v^2 \quad \text{and} \quad \frac{bv^1 - av^2}{v^1 - v^2} < \alpha < \frac{av^1 - bv^2}{v^1 - v^2} \quad \text{if} \quad v^1 > v^2; \quad (5)$$

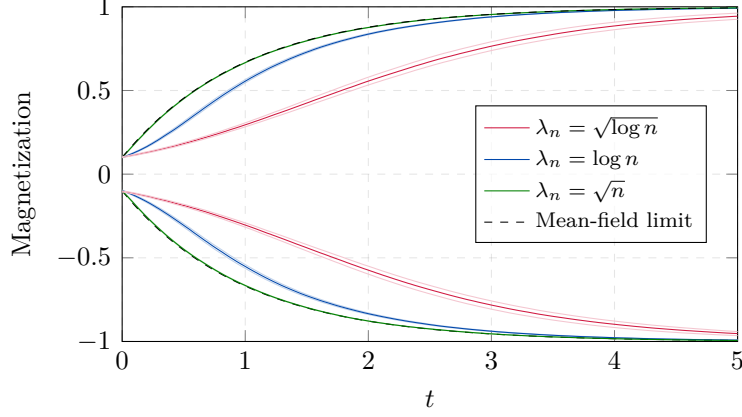


Figure 1: The dashed curves show the mean-field limit, each of the dark solid curves was obtained by averaging the results of 100 simulations and the light solid curves show 95% confidence intervals around the dark solid curves; the positive curves correspond to z_n^1 and the negative curves to z_n^2 . The values of λ_n in the legend are ordered from inner curves to outer curves. In all the cases both communities have size $n = 5000$, $a = 5$, $b = 1$, $\eta = 0.1$, $\alpha = 0$ and $\beta_n = \infty$.

α can take any real value if $v^1 = v^2$. Fix $\eta \in (0, 1]$ and a sequence $\beta_n \in (0, \infty]$ such that

$$\lim_{n \rightarrow \infty} \beta_n \lambda_n = \infty. \quad (6)$$

Then $z_n \Rightarrow z_\infty$ in $D_{\mathbb{R}^2}[0, \infty)$ as $n \rightarrow \infty$, where z_∞ is the unique function such that

$$z_\infty^k(0) = \begin{cases} \eta & \text{if } k = 1, \\ -\eta & \text{if } k = 2, \end{cases} \quad \text{and} \quad \dot{z}_\infty^k(t) = \begin{cases} 1 - z_\infty^k(t) & \text{if } k = 1, \\ -1 - z_\infty^k(t) & \text{if } k = 2, \end{cases} \quad \text{for all } t \geq 0.$$

Moreover, if the sequence $\gamma_n > 0$ is such that

$$\lim_{n \rightarrow \infty} \frac{\gamma_n}{\sqrt{n}} = 0, \quad \lim_{n \rightarrow \infty} \frac{\gamma_n}{\lambda_n} = 0 \quad \text{and} \quad \lim_{n \rightarrow \infty} \gamma_n e^{-\beta_n \lambda_n} = 0, \quad (7)$$

then $\gamma_n(z_n - z_\infty) \Rightarrow 0$ in $D_{\mathbb{R}^2}[0, \infty)$ as $n \rightarrow \infty$.

As observed in Section 1, the situation where $\alpha = 0$ and $\beta_n = \infty$ for all n corresponds to the Label Propagation or Majority Vote algorithm, which had not been rigorously analyzed before. The plot shown in Figure 1 corresponds to the latter choice of hyperparameters and illustrates how the convergence rate to the mean-field limit depends on λ_n , as is also captured by (7). In particular, for graphs of the same finite size, the trajectories of z_n get closer to the mean-field limit when the graph is denser.

Remark 2. If the graph is fixed, then a nonasymptotic version of (5) is given by

$$\frac{b_n V_n^1 - a_n V_n^2}{V_n^1 - V_n^2} < \alpha_n < \frac{a_n V_n^1 - b_n V_n^2}{V_n^1 - V_n^2} \quad \text{if } V_n^1 > V_n^2.$$

While this condition depends on the possibly unknown community sizes and edge densities,

these quantities can be easily estimated by considering the fraction η of revealed labels. The community sizes can be estimated by counting the number of revealed labels in each community, while the edge densities can be estimated by counting the numbers of edges between nodes with revealed labels in the same community or in different communities.

Remark 3. Suppose that, similarly to the setting of [4], the oracle makes mistakes for nodes in \mathcal{V}_n^k with probability q^k . Then the average magnetization when the algorithm starts is given by $\eta - 2\eta q^1$ for \mathcal{V}_n^1 and $-\eta + 2\eta q^2$ for \mathcal{V}_n^2 . Theorems 1 and 2, stated below, can be extended to the situation where the oracle makes mistakes, provided that:

$$\begin{aligned} (a - \alpha) v^1 (\eta - 2\eta q^1) + (b - \alpha) v^2 (-\eta + 2\eta q^2) &> 0, \\ (b - \alpha) v^1 (\eta - 2\eta q^1) + (a - \alpha) v^2 (-\eta + 2\eta q^2) &< 0; \end{aligned}$$

observe that if $q^1 = 0 = q^2$, then we recover condition (5). The proofs follow from similar arguments as in the case without mistakes, by noting that the above conditions imply that the point $(\eta - 2\eta q^1, -\eta + 2\eta q^2)$ is in the interior of the gray set depicted in Figure 2.

It is straightforward to check that the mean-field limit \mathbf{z}_∞ is such that

$$\mathbf{z}_\infty^1(t) = 1 + (\eta - 1)e^{-t} = -\mathbf{z}_\infty^2(t) \quad \text{for all } t \geq 0. \quad (8)$$

As a result, $\mathbf{z}_\infty^1(t) \rightarrow 1$ and $\mathbf{z}_\infty^2(t) \rightarrow -1$ as $t \rightarrow \infty$, which corresponds to the spin being constant within each community and opposite between communities. If γ_n satisfies (7) and t is a fixed time, then Theorem 1 and (8) imply that

$$\max \left\{ \left| \mathbf{z}_n^1(t) - 1 \right|, \left| \mathbf{z}_n^2(t) + 1 \right| \right\} = (1 - \eta)e^{-t} + o\left(\frac{1}{\gamma_n}\right). \quad (9)$$

In practice, this expression can be used to select the simulation time t_{end} required as input in Algorithm 1, e.g., in a way that keeps the relative classification error below a given threshold. If $t_{\text{end}} > \log[2(1 - \eta)/\varepsilon]$, then the first term on the right-hand side is smaller than $\varepsilon/2$ and thus the relative error is less than ε if the graph is large enough.

The expression (9) also suggests that we may achieve almost exact recovery, i.e., a vanishing fraction of misclassified nodes, if the simulation time $t_{\text{end}} = t_n$ approaches infinity as $n \rightarrow \infty$. Observe that this does not follow directly from the limits stated in Theorem 1 since these limits hold with respect to the topology of uniform convergence over compact sets. Nonetheless, we prove in Section 6 that almost exact recovery is indeed achieved if $t_n \rightarrow \infty$ as $n \rightarrow \infty$ in the way stated in the following theorem.

Theorem 2. Assume that (5) holds. Fix $\eta \in (0, 1]$ and a sequence $\beta_n \in (0, \infty]$ such that

$$\lim_{n \rightarrow \infty} \frac{\beta_n \lambda_n}{\log \lambda_n} = \infty. \quad (10)$$

If $t_n := c \log \lambda_n$ with $0 < c < 1/4$, and the above conditions hold, then

$$\max \left\{ \left| \mathbf{z}_n^1(t_n) - 1 \right|, \left| \mathbf{z}_n^2(t_n) + 1 \right| \right\} \Rightarrow 0 \quad \text{as } n \rightarrow \infty. \quad (11)$$

Moreover, the limit holds in expectation as well.

The Glauber dynamics used in Algorithm 1 flip each spin at most at unit rate, which means that some spin flips at rate $O(n)$. It follows that the average number of flips when the dynamics are simulated for t_n units of time is $O(nt_n) = O(n \log \lambda_n)$, which is quasi-linear in the size of the graph. Theorem 2 says that this is enough for almost exact recovery.

Remark 4. We require that $t_n < (\log \lambda_n)/4$ for technical reasons, but believe that almost exact recovery is also achieved if t_n grows faster. However, almost exact recovery may not hold if t_n grows too fast. If $\alpha = 0$, then the stationary distribution of σ_n given by (2) assigns the highest probability to the configurations with constant spin. Thus, if t_n grows fast enough, faster than the mixing time of σ_n , then almost exact recovery does not hold.

4 Mean-field approximation

Using standard arguments, we may construct the Markov chain σ_n such that:

$$\begin{aligned} \mathbf{z}_n^k(t) - \mathbf{z}_n^k(0) = & \frac{2}{V_n^k} \mathcal{N}_+^k \left(\int_0^t \sum_{u \in \mathcal{Y}_-^k(\sigma_n(\tau))} r(\beta_n \Delta_n(\sigma_n(\tau), u)) d\tau \right) \\ & - \frac{2}{V_n^k} \mathcal{N}_-^k \left(\int_0^t \sum_{u \in \mathcal{Y}_+^k(\sigma_n(\tau))} r(\beta_n \Delta_n(\sigma_n(\tau), u)) d\tau \right) \quad \text{for all } t \geq 0, \end{aligned}$$

where the processes \mathcal{N}_s^k are independent Poisson processes with unit rates. The sum in the first line is the rate at which a negative spin in \mathcal{V}_n^k flips, and the sum in the second line is the rate at which a positive spin flips. The former situation increases \mathbf{z}_n^k by $2/V_n^k$,

whereas the latter situation decreases z_n^k by the same amount. Let

$$\begin{aligned} \mathcal{M}_n^k(t) &= \mathcal{N}_+^k \left(\int_0^t \sum_{u \in \mathcal{V}_-^k(\sigma_n(\tau))} r(\beta_n \Delta_n(\sigma_n(\tau), u)) d\tau \right) \\ &\quad - \mathcal{N}_-^k \left(\int_0^t \sum_{u \in \mathcal{V}_+^k(\sigma_n(\tau))} r(\beta_n \Delta_n(\sigma_n(\tau), u)) d\tau \right) \\ &\quad + \int_0^t \sum_{u \in \mathcal{V}_n^k} \sigma_n(\tau, u) r(\beta_n \Delta_n(\sigma_n(\tau), u)) d\tau, \end{aligned}$$

which is the sum of two centered Poisson processes. Then we may write

$$z_n^k(t) = z_n^k(0) + \frac{2}{V_n^k} \mathcal{M}_n^k(t) - \frac{2}{V_n^k} \int_0^t \sum_{u \in \mathcal{V}_n^k} \sigma_n(\tau, u) r(\beta_n \Delta_n(\sigma_n(\tau), u)) d\tau. \quad (12)$$

The energy variation in σ when the spin of $u \in \mathcal{V}_n^k$ flips can be expressed as follows:

$$\begin{aligned} \Delta_n(\sigma, u) &= 2\sigma(u) \left[\sum_{v \sim u} \sigma(v) - \alpha_n \sum_{l=1,2} \sum_{v \in \mathcal{V}_n^l} \sigma(v) \right] + 2\alpha_n \\ &= 2\sigma(u) \sum_{l=1,2} \left[\sum_{v \in \mathcal{N}_n^l(u)} \sigma(v) - \alpha_n V_n^l z^l(\sigma) \right] + 2\alpha_n. \end{aligned} \quad (13)$$

If we let $\bar{k} := 3 - k$, then it makes sense to approximate

$$\sum_{v \in \mathcal{N}_n^k(u)} \sigma_n(t, v) \quad \text{by} \quad a_n V_n^k z_n^k(t) \quad \text{and} \quad \sum_{v \in \mathcal{N}_n^{\bar{k}}(u)} \sigma_n(t, v) \quad \text{by} \quad b_n V_n^{\bar{k}} z_n^{\bar{k}}(t).$$

The right-hand sides would be the expected values of the left-hand sides if $\sigma_n(t)$ and \mathcal{G}_n were independent, but they are not independent for $t > 0$ because the Glauber dynamics depend on the graph structure. Consider the linear function $\mathcal{L}^k : \mathbb{R}^2 \rightarrow \mathbb{R}$ such that

$$\mathcal{L}^k(z) := (a - \alpha) v^k z^k + (b - \alpha) v^{\bar{k}} z^{\bar{k}} \quad \text{for all } z \in \mathbb{R}^2.$$

If we drop the last term of (13) and we further approximate the coefficients $a_n V_n^k$, $b_n V_n^{\bar{k}}$ and $\alpha_n V_n^k$ by $av^k \lambda_n$, $bv^{\bar{k}} \lambda_n$ and $\alpha v^k \lambda_n$, respectively, then we may approximate

$$\Delta_n(\sigma_n(t), u) \quad \text{by} \quad 2\lambda_n \sigma_n(t, u) \mathcal{L}^k(z_n(t)) \quad \text{for } u \in \mathcal{V}_n^k.$$

It is not difficult to check that

$$\frac{Y_+^k(\sigma_n)}{V_n^k} = \frac{1 + z_n^k}{2} \quad \text{and} \quad \frac{Y_-^k(\sigma_n)}{V_n^k} = \frac{1 - z_n^k}{2}.$$

Indeed, the sum of the quantities on the left equals one and their difference is z_n^k . Further, $r(x) + r(-x) = 1$ and $r(2x) - r(-2x) = -\tanh(x)$ for all $x \in \mathbb{R}$. Thus,

$$\begin{aligned} \frac{2}{V_n^k} \sum_{u \in \mathcal{V}_n^k} \sigma_n(u) r(\beta_n \Delta_n(\sigma_n, u)) &= \frac{2}{V_n^k} \sum_{u \in \mathcal{V}_+^k(\sigma_n)} \left[r(\beta_n \Delta_n(\sigma_n, u)) - r(2\beta_n \lambda_n \mathcal{L}^k(z_n)) \right] \\ &\quad - \frac{2}{V_n^k} \sum_{u \in \mathcal{V}_-^k(\sigma_n)} \left[r(\beta_n \Delta_n(\sigma_n, u)) - r(-2\beta_n \lambda_n \mathcal{L}^k(z_n)) \right] \\ &\quad - \tanh(\beta_n \lambda_n \mathcal{L}^k(z_n)) + z_n^k. \end{aligned}$$

We conclude from the latter equation and (12) that

$$\begin{aligned} z_n^k(t) &= z_n^k(0) + \int_0^t \left[\tanh(\beta_n \lambda_n \mathcal{L}^k(z_n(\tau))) - z_n^k(\tau) \right] d\tau + \frac{2}{V_n^k} \mathcal{M}_n^k(t) \\ &\quad - \frac{2}{V_n^k} \int_0^t \sum_{u \in \mathcal{V}_n^k} \left[r(\beta_n \Delta_n(\sigma_n(\tau), u)) - r(2\beta_n \lambda_n \sigma_n(\tau, u) \mathcal{L}^k(z_n(\tau))) \right] d\tau. \end{aligned} \quad (14)$$

The first two terms are what we call the mean-field approximation. The last two terms are the errors associated with this approximation and will be shown to vanish as $n \rightarrow \infty$. It follows from (4) that the above equation holds with

$$\tanh(\beta_n x) = r(-2\beta_n x) - r(2\beta_n x) = \text{sign}(x) \quad \text{for all } x \in \mathbb{R} \quad \text{if } \beta_n = \infty.$$

For each configuration $\sigma \in \Sigma_n$, define

$$\mathcal{E}^k(\sigma) := \frac{2}{V_n^k} \sum_{u \in \mathcal{V}_n^k} \left[r(\beta_n \Delta_n(\sigma, u)) - r(2\beta_n \lambda_n \sigma(u) \mathcal{L}^k(z(\sigma))) \right].$$

Using this notation, we may rewrite (14) as follows:

$$z_n^k(t) = z_n^k(0) + \int_0^t \left[\tanh(\beta_n \lambda_n \mathcal{L}^k(z_n(\tau))) - z_n^k(\tau) - \mathcal{E}^k(\sigma_n(\tau)) \right] d\tau + \frac{2}{V_n^k} \mathcal{M}_n^k(t). \quad (15)$$

5 Proof of Theorem 1

In this section we prove Theorem 1. The first step is to prove a tightness result which implies that every convergent subsequence of $\{z_n : n \geq 1\}$ has a further subsequence that converges weakly in $D_{\mathbb{R}^2}[0, \infty)$. By standard arguments, it then suffices to fix an arbitrary convergent subsequence $\{z_m : m \in \mathcal{M}\}$ and prove that $z_m \Rightarrow z_\infty$ and $\gamma_m(z_m - z_\infty) \Rightarrow 0$ in $D_{\mathbb{R}^2}[0, \infty)$ as $m \rightarrow \infty$ under the corresponding assumptions in Theorem 1. Furthermore, it is enough to fix an arbitrary $T \geq 0$ and prove the limits for the uniform metric over the finite interval $[0, T]$. A key step for this, which is deferred until Section 7, is to show that the last two terms of (14) converge weakly to zero. In particular, Proposition 3 is where

we overcome the main obstacle created by the mutual dependence between the current spin configuration and the structure of the random graph. Finally, we invoke Skorohod's representation theorem to obtain versions of the processes such that the convergence holds almost surely, and prove that almost all trajectories satisfy $\mathbf{z}_m \rightarrow \mathbf{z}_\infty$ and $\gamma_m(\mathbf{z}_m - \mathbf{z}_\infty) \rightarrow 0$ uniformly over $[0, T]$ as $m \rightarrow \infty$ under the corresponding assumptions.

The tightness result is stated below and proved in Appendix A, using the fact that the processes \mathbf{z}_n have jumps of size $O(1/n)$ at rate $O(n)$.

Lemma 1. *The sequence of processes $\{\mathbf{z}_n : n \geq 1\}$ is tight in $D_{\mathbb{R}^2}[0, \infty)$ with respect to the topology of uniform convergence over compact sets, and every subsequence of $\{\mathbf{z}_n : n \geq 1\}$ has a further subsequence that converges weakly to an almost surely continuous process.*

Consider any sequence $\mathcal{M} \subset \mathbb{N}$ such that $\mathbf{z}_m \Rightarrow \mathbf{z}$ in $D_{\mathbb{R}^2}[0, \infty)$ as $m \rightarrow \infty$, where \mathbf{z} is almost surely continuous and m takes values in \mathcal{M} . In order to establish Theorem 1, it suffices to show that the following two properties hold for any such sequence:

- (a) $\mathbf{z} = \mathbf{z}_\infty$ with probability one if (5) and (6) hold,
- (b) $\gamma_m(\mathbf{z}_m - \mathbf{z}_\infty) \Rightarrow 0$ in $D_{\mathbb{R}^2}[0, \infty)$ as $m \rightarrow \infty$ if (7) holds as well.

Property (a) can be proved by showing that for each $T \geq 0$, we have $\mathbf{z}(t) = \mathbf{z}_\infty(t)$ for all $t \in [0, T]$ almost surely. Similarly, let $D_{\mathbb{R}^2}[0, T]$ be the space of càdlàg functions from $[0, T]$ into \mathbb{R} with the topology of uniform convergence. Then (b) holds if $\gamma_m(\mathbf{z}_m - \mathbf{z}_\infty) \Rightarrow 0$ in $D_{\mathbb{R}^2}[0, T]$ as $m \rightarrow \infty$ for all $T \geq 0$. Thus, we fix $T \geq 0$ and prove these properties.

For each $\xi \in (0, 1)$ and $\zeta > 0$, consider the following sets:

$$\begin{aligned} \mathcal{A}(\zeta, \xi) &:= \left\{ z \in [-1 + \xi, 1 - \xi]^2 : \min \left\{ \mathcal{L}^1(z), -\mathcal{L}^2(z) \right\} \geq \zeta \right\}, \\ \Sigma_n(\zeta, \xi) &:= \left\{ \sigma \in \Sigma_n : z(\sigma) \in \mathcal{A}(\zeta, \xi) \right\}. \end{aligned}$$

The former set is depicted in Figure 2. The value of $\tanh(\beta_n \lambda_n \mathcal{L}^k(\mathbf{z}_n))$ in (15) is mostly given by the sign of $\mathcal{L}^k(\mathbf{z}_n)$, particularly when $\beta_n \lambda_n$ is large, and this sign depends on the position of \mathbf{z}_n relative to the line $\mathcal{L}^k(z) = 0$ plotted in Figure 2. We have $\mathcal{L}^1(\mathbf{z}_n) > 0$ and $\mathcal{L}^2(\mathbf{z}_n) < 0$ when \mathbf{z}_n is in the interior of the set $\mathcal{A}(0, 0)$, and this pushes \mathbf{z}_n in the direction of the point $(1, -1)$, which is such that the spins are positive in \mathcal{V}_n^1 and negative in \mathcal{V}_n^2 .

It follows from (8) that

$$0 < \eta \leq \mathbf{z}_\infty^1(t) = -\mathbf{z}_\infty^2(t) \leq 1 + (\eta - 1)e^{-T} < 1 \quad \text{for all } t \in [0, T].$$

We conclude from the above relations and condition (5) that

$$\begin{aligned} \mathcal{L}^1(\mathbf{z}_\infty(t)) &= \left[(a - \alpha)v^1 - (b - \alpha)v^2 \right] \mathbf{z}_\infty^1(t) \geq \mathcal{L}^1(\mathbf{z}_\infty(0)) = \left[(a - \alpha)v^1 - (b - \alpha)v^2 \right] \eta > 0, \\ \mathcal{L}^2(\mathbf{z}_\infty(t)) &= \left[(b - \alpha)v^1 - (a - \alpha)v^2 \right] \mathbf{z}_\infty^1(t) \leq \mathcal{L}^2(\mathbf{z}_\infty(0)) = \left[(b - \alpha)v^2 - (a - \alpha)v^1 \right] \eta < 0, \end{aligned}$$

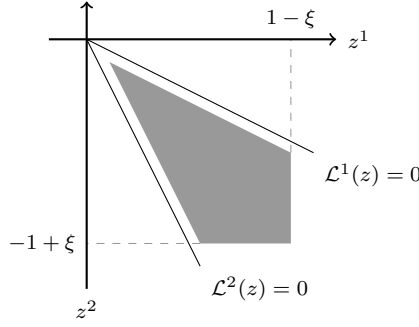


Figure 2: The shaded region represents the set $\mathcal{A}(\zeta, \xi)$ when condition (5) holds and $\alpha > a$. The slopes of the lines $\mathcal{L}^1(z) = 0$ and $\mathcal{L}^2(z) = 0$ depend on the value of α as illustrated in Figure 3 of Section 8.

for all $t \geq 0$. In particular, we may write

$$\min \left\{ \mathcal{L}^1(z_\infty(t)), -\mathcal{L}^2(z_\infty(t)) \right\} \geq \min \left\{ \mathcal{L}^1(z_\infty(0)), -\mathcal{L}^2(z_\infty(0)) \right\} > 0. \quad (16)$$

Then there exists $\theta \in (0, 1)$ such that $z_\infty(t)$ is in the interior of $\mathcal{A}(\theta, \theta)$ for all $t \in [0, T]$.

If (5) and (6) hold and $\gamma_m = 1$ for all $m \in \mathcal{M}$, or if (5), (6) and (7) hold, then:

$$z_m \Rightarrow z \quad \text{in} \quad D_{\mathbb{R}^2}[0, T], \quad (17a)$$

$$\gamma_m \left(\frac{\mathcal{M}_m^1}{V_m^1}, \frac{\mathcal{M}_m^2}{V_m^2} \right) \Rightarrow 0 \quad \text{in} \quad D_{\mathbb{R}^2}[0, T], \quad (17b)$$

$$\gamma_m [z_m(0) - z_\infty(0)] \Rightarrow 0 \quad \text{in} \quad \mathbb{R}^2, \quad (17c)$$

$$\gamma_m \left(\max_{\sigma \in \Sigma_m(\theta, \theta)} \mathcal{E}^1(\sigma), \max_{\sigma \in \Sigma_m(\theta, \theta)} \mathcal{E}^2(\sigma) \right) \Rightarrow 0 \quad \text{in} \quad \mathbb{R}^2, \quad (17d)$$

as $m \rightarrow \infty$. The first limit holds because we are considering a convergent subsequence. The second limit is essentially a consequence of the central limit theorem for the Poisson process and is proved in Proposition 2 of Section 7. The third limit follows from the central limit theorem for independent and identically distributed random variables and is derived in Lemma 7 of Appendix C. The fourth limit is obtained in Proposition 3 of Section 7 using concentration inequalities for the binomial distribution.

Lemma 2. *The graphs \mathcal{G}_m , the processes introduced in Section 4 and the process z can be constructed on a common probability space $(\Omega, \mathcal{F}, \mathbb{P})$ for all $m \in \mathcal{M}$ such that the following limits hold as $m \rightarrow \infty$ with probability one:*

$$z_m \rightarrow z \quad \text{in} \quad D_{\mathbb{R}^2}[0, T], \quad (18a)$$

$$\gamma_m \left(\frac{\mathcal{M}_m^1}{V_m^1}, \frac{\mathcal{M}_m^2}{V_m^2} \right) \rightarrow 0 \quad \text{in} \quad D_{\mathbb{R}^2}[0, T], \quad (18b)$$

$$\gamma_m [z_m(0) - z_\infty(0)] \rightarrow 0 \quad \text{in} \quad \mathbb{R}^2, \quad (18c)$$

$$\gamma_m \left(\max_{\sigma \in \Sigma_m(\theta, \theta)} \mathcal{E}^1(\sigma), \max_{\sigma \in \Sigma_m(\theta, \theta)} \mathcal{E}^2(\sigma) \right) \rightarrow 0 \quad \text{in} \quad \mathbb{R}^2. \quad (18d)$$

The above technical lemma is proved in Appendix C using Skorohod's representation theorem. In order to prove Theorem 1, it remains to establish that Ω contains a subset of probability one such that all ω in this subset satisfy the following properties:

(a') $\mathbf{z}(\omega, t) = \mathbf{z}_\infty(t)$ for all $t \in [0, T]$ when (5) and (6) hold,

(b') $\gamma_m [\mathbf{z}_m(\omega) - \mathbf{z}_\infty] \rightarrow 0$ in $D_{\mathbb{R}^2}[0, T]$ as $m \rightarrow \infty$ when (7) holds as well.

Below we establish that the above properties hold for all ω in the set of probability one where (18) holds and $\mathbf{z}(\omega)$ is continuous.

Proof of property (a')

Fix any ω such that (18) holds and $\mathbf{z}(\omega)$ is continuous; in the sequel we will omit ω from the notation for brevity. In addition, consider the time defined as

$$\tau := \inf \{t \in [0, T] : \mathbf{z}(t) \neq \mathbf{z}_\infty(t)\}. \quad (19)$$

If $\tau = T$, then (a') holds, so assume that $\tau < T$. Note that \mathbf{z} is continuous and $\mathbf{z}_m \rightarrow \mathbf{z}$ uniformly over $[0, T]$ as $m \rightarrow \infty$. Hence, there exist $\varepsilon > 0$ and $m_0 \geq 1$ such that

$$\mathbf{z}_m(t) \in \mathcal{A}(\theta, \theta) \quad \text{for all } t \in [0, \tau + \varepsilon] \quad \text{and} \quad m \in \mathcal{M} \quad \text{with} \quad m \geq m_0. \quad (20)$$

For all $c > 0$ and $x > \theta$, we have

$$|-1 - \tanh(-cx)| = |1 - \tanh(cx)| = 1 - \frac{e^{cx} - e^{-cx}}{e^{cx} + e^{-cx}} \leq 2e^{-c\theta}. \quad (21)$$

The above inequality, (6), (18d) and (20) imply that

$$\begin{aligned} \lim_{m \rightarrow \infty} \sup_{t \in [0, \tau + \varepsilon]} \left| \tanh \left(\beta_m \lambda_m \mathcal{L}^k(\mathbf{z}_m(t)) \right) - \mathbb{1}_{\{k=1\}} + \mathbb{1}_{\{k=2\}} \right| &= 0, \\ \lim_{m \rightarrow \infty} \sup_{t \in [0, \tau + \varepsilon]} \mathcal{E}^k(\boldsymbol{\sigma}_m(t)) &\leq \lim_{m \rightarrow \infty} \max_{\sigma \in \Sigma_m(\theta, \theta)} \mathcal{E}^k(\sigma) = 0. \end{aligned}$$

If we replace the hyperbolic tangent in the first limit by a sign function, then the limit still holds, which covers the case $\beta_m = \infty$. Now it follows from (15) and (18) that

$$\mathbf{z}^k(t) = \mathbf{z}_\infty^k(0) + \int_0^t \left[\mathbb{1}_{\{k=1\}} - \mathbb{1}_{\{k=2\}} - \mathbf{z}^k(\zeta) \right] d\zeta \quad \text{for all } t \in [0, \tau + \varepsilon] \quad \text{and} \quad k \in \{1, 2\}.$$

Then $\mathbf{z}(t) = \mathbf{z}_\infty(t)$ for all $t \in [0, \tau + \varepsilon]$ contradicting (19), so (a') must hold.

Proof of property (b')

Suppose that (7) holds and fix any ω such that (18) holds and $\mathbf{z}(\omega)$ is continuous; we omit ω from the notation for brevity. Since (a') holds, by similar arguments as for (20),

there exists $m_1 \geq 1$ such that

$$\mathbf{z}_m(t) \in \mathcal{A}(\theta, \theta) \quad \text{for all } t \in [0, T] \quad \text{and } m \in \mathcal{M} \quad \text{with } m \geq m_1.$$

Then it follows from (7), (18d) and (21) that the following limits hold:

$$\begin{aligned} \lim_{m \rightarrow \infty} \sup_{t \in [0, T]} \gamma_m \left| \tanh \left(\beta_m \lambda_m \mathcal{L}^k(\mathbf{z}_m(t)) \right) - \left(\mathbb{1}_{\{k=1\}} - \mathbb{1}_{\{k=2\}} \right) \right| &= 0, \\ \lim_{m \rightarrow \infty} \sup_{t \in [0, T]} \gamma_m \mathcal{E}^k(\boldsymbol{\sigma}_m(t)) &\leq \lim_{m \rightarrow \infty} \max_{\sigma \in \Sigma_m(\theta, \theta)} \gamma_m \mathcal{E}^k(\sigma) = 0. \end{aligned} \quad (22)$$

Let $\mathbf{d}_m^k(t) := \gamma_m |\mathbf{z}_m^k(t) - \mathbf{z}_\infty^k(t)|$. The definition of \mathbf{z}_∞ and (15) imply that

$$\begin{aligned} \mathbf{d}_m^k(t) &\leq \mathbf{d}_m^k(0) + \int_0^t \gamma_m \left| \mathcal{E}^k(\boldsymbol{\sigma}_m(\zeta)) \right| d\zeta + \frac{2\gamma_m}{V_m^k} \left| \mathcal{M}_m^k(t) \right| \\ &\quad + \int_0^t \gamma_m \left| \tanh \left(\beta_m \lambda_m \mathcal{L}^k(\mathbf{z}_m(\zeta)) \right) - \mathbb{1}_{\{k=1\}} + \mathbb{1}_{\{k=2\}} \right| d\zeta + \int_0^t \mathbf{d}_m^k(\zeta) d\zeta \end{aligned}$$

for all $t \in [0, T]$. Taking the supremum over $s \in [0, t]$ on both sides, we obtain:

$$\begin{aligned} \sup_{s \in [0, t]} \mathbf{d}_m^k(s) &\leq \mathbf{d}_m^k(0) + t \sup_{s \in [0, t]} \gamma_m \left| \mathcal{E}^k(\boldsymbol{\sigma}_m(s)) \right| + \sup_{s \in [0, t]} \frac{2\gamma_m}{V_m^k} \left| \mathcal{M}_m^k(s) \right| \\ &\quad + t \sup_{s \in [0, t]} \gamma_m \left| \tanh \left(\beta_m \lambda_m \mathcal{L}^k(\mathbf{z}_m(s)) \right) - \mathbb{1}_{\{k=1\}} + \mathbb{1}_{\{k=2\}} \right| + \int_0^t \sup_{s \in [0, \zeta]} \mathbf{d}_m^k(s) d\zeta. \end{aligned} \quad (23)$$

For brevity, let us write

$$\begin{aligned} \varepsilon_m^k &:= \mathbf{d}_m^k(0) + T \sup_{t \in [0, T]} \gamma_m \left| \mathcal{E}^k(\boldsymbol{\sigma}_m(t)) \right| + \sup_{t \in [0, T]} \frac{2\gamma_m}{V_m^k} \left| \mathcal{M}_m^k(t) \right| \\ &\quad + T \sup_{t \in [0, T]} \gamma_m \left| \tanh \left(\beta_m \lambda_m \mathcal{L}^k(\mathbf{z}_m(t)) \right) - \mathbb{1}_{\{k=1\}} + \mathbb{1}_{\{k=2\}} \right|. \end{aligned}$$

We conclude from Grönwall's inequality, (18b), (18c) and (22) that

$$\lim_{m \rightarrow \infty} \sup_{t \in [0, T]} \mathbf{d}_m^k(t) \leq \lim_{m \rightarrow \infty} \varepsilon_m^k e^T = 0.$$

This proves that (b') holds and therefore completes the proof of Theorem 1.

6 Proof of Theorem 2

In this section we prove Theorem 2. By (8) and the triangular inequality,

$$\max \left\{ \left| \mathbf{z}_n^1(t_n) - 1 \right|, \left| \mathbf{z}_n^2(t_n) + 1 \right| \right\} \leq \frac{1 - \eta}{\lambda_n^c} + \max_{k=1,2} \mathbf{d}_n^k(t_n),$$

where $\mathbf{d}_n^k(t) := |\mathbf{z}_n^k(t) - \mathbf{z}_\infty^k(t)|$ for all $t \geq 0$. Therefore, it suffices to show that

$$\max_{k=1,2} \mathbf{d}_n^k(t_n) \Rightarrow 0 \quad \text{as } n \rightarrow \infty.$$

Note that $\mathbf{d}_n^k(t)$ is as in Section 5 with $\gamma_n = 1$. However, in Section 5 the variable t ranged in a fixed interval $[0, T]$ for all n , whereas here t ranges in $[0, t_n]$ and $t_n \rightarrow \infty$ as $n \rightarrow \infty$. Hence, we must resort to different arguments to prove the above limit.

It follows from (5) that (16) holds for all $t \geq 0$, so we can take $\zeta > 0$ such that

$$\min \left\{ \mathcal{L}^1(\mathbf{z}_\infty(t)), -\mathcal{L}^2(\mathbf{z}_\infty(t)) \right\} \geq \min \left\{ \mathcal{L}^1(\mathbf{z}_\infty(0)), -\mathcal{L}^2(\mathbf{z}_\infty(0)) \right\} > \zeta \quad \text{for all } t \geq 0.$$

Let us fix some $d \in (c, 1 - 2c)$ and define the following constant and random time:

$$\xi_n := \frac{1}{\lambda_n^d} \quad \text{and} \quad \tau_n := \min \{t_n, \inf \{t \geq 0 : \mathbf{z}_n(t) \notin \mathcal{A}(\zeta, \xi_n)\}\}.$$

By definition of ζ and the linearity of \mathcal{L}^1 and \mathcal{L}^2 , there exists $\theta > 0$ such that

$$\max_{k=1,2} \mathbf{d}_n^k(t) \leq \theta \quad \text{implies that} \quad \min \left\{ \mathcal{L}^1(\mathbf{z}_n(t)), -\mathcal{L}^2(\mathbf{z}_n(t)) \right\} \geq \zeta.$$

By (8), we have $\mathbf{z}_n^1(t) \leq \mathbf{z}_\infty^1(t) + \mathbf{d}_n^1(t) = 1 + (\eta - 1)e^{-t} + \mathbf{d}_n^1(t)$. Thus, $[\xi_n + \mathbf{d}_n^1(t)]e^t \leq 1 - \eta$ gives $\mathbf{z}_n^1(t) \leq 1 - \xi_n$. Using similar arguments, we obtain:

$$\left[\xi_n + \max_{k=1,2} \mathbf{d}_n^k(t) \right] e^t \leq 1 - \eta \quad \text{implies that} \quad \mathbf{z}_n(t) \in [-1 + \xi_n, 1 - \xi_n]^2.$$

Combining the two observations, we conclude that

$$\max_{k=1,2} \mathbf{d}_n^k(t) \leq \theta \quad \text{and} \quad \left[\xi_n + \max_{k=1,2} \mathbf{d}_n^k(t) \right] e^t \leq 1 - \eta \quad \text{imply that} \quad \mathbf{z}_n(t) \in \mathcal{A}(\zeta, \xi_n).$$

In order to prove (11), it suffices to show that

$$\left[\xi_n + \max_{k=1,2} \sup_{t \in [0, \tau_n]} \mathbf{d}_n^k(t) \right] e^{t_n} \Rightarrow 0 \quad \text{as } n \rightarrow \infty. \quad (24)$$

Indeed, $(1 - \eta)e^{-t_n} \leq \theta$ for all sufficiently large n , and thus

$$\left[\xi_n + \max_{k=1,2} \sup_{t \in [0, \tau_n]} \mathbf{d}_n^k(t) \right] e^{t_n} \leq 1 - \eta \quad \text{implies that} \quad \mathbf{z}_n(t) \in \mathcal{A}(\zeta, \xi_n) \quad \text{for all } t \in [0, \tau_n].$$

Note that $\mathbf{z}_n(t) \in \mathcal{A}(\zeta, \xi_n)$ for all $t \in [0, \tau_n]$ implies that $\tau_n = t_n$. Hence, (24) yields

$$\lim_{n \rightarrow \infty} P \left(\left[\xi_n + \max_{k=1,2} \sup_{t \in [0, t_n]} \mathbf{d}_n^k(t) \right] e^{t_n} < \varepsilon \right) = \lim_{n \rightarrow \infty} P \left(\left[\xi_n + \max_{k=1,2} \sup_{t \in [0, \tau_n]} \mathbf{d}_n^k(t) \right] e^{t_n} < \varepsilon \right) = 1$$

if $0 < \varepsilon \leq 1 - \eta$. Thus, (24) implies (11), because the above limit implies that

$$\max_{k=1,2} \mathbf{d}_n^k(t_n) \leq \left[\xi_n + \max_{k=1,2} \sup_{t \in [0, t_n]} \mathbf{d}_n^k(t) \right] e^{t_n} \Rightarrow 0 \quad \text{as } n \rightarrow \infty.$$

We proceed with the proof of (24). As in (23), we obtain:

$$\begin{aligned} \sup_{s \in [0, t]} \mathbf{d}_n^k(s) &\leq \mathbf{d}_n^k(0) + t \sup_{s \in [0, t]} \left| \mathcal{E}^k(\boldsymbol{\sigma}_n(s)) \right| + \sup_{s \in [0, t]} \frac{2}{V_n^k} \left| \mathcal{M}_n^k(s) \right| \\ &\quad + t \sup_{s \in [0, t]} \left| \tanh \left(\beta_n \lambda_n \mathcal{L}^k(\mathbf{z}_n(s)) \right) - \mathbb{1}_{\{k=1\}} + \mathbb{1}_{\{k=2\}} \right| + \int_0^t \sup_{s \in [0, \tau]} \mathbf{d}_n^k(s) d\tau \end{aligned}$$

for all $t \geq 0$. For brevity, let us introduce the following notation:

$$\begin{aligned} \mathbf{f}_n^k(t) &:= \mathbf{d}_n^k(0) + \sup_{s \in [0, t]} \frac{2}{V_n^k} \left| \mathcal{M}_n^k(s) \right| \\ \mathbf{g}_n^k(t) &:= \sup_{s \in [0, t]} \left| \mathcal{E}^k(\boldsymbol{\sigma}_n(s)) \right| + \sup_{s \in [0, t]} \left| \tanh \left(\beta_n \lambda_n \mathcal{L}^k(\mathbf{z}_n(s)) \right) - \mathbb{1}_{\{k=1\}} + \mathbb{1}_{\{k=2\}} \right|. \end{aligned}$$

It follows from Grönwall's inequality and $\tau_n \leq t_n = c \log \lambda_n$ that

$$\sup_{t \in [0, \tau_n]} \mathbf{d}_n^k(t) \leq \left[\mathbf{f}_n^k(\tau_n) + \tau_n \mathbf{g}_n^k(\tau_n) \right] e^{\tau_n} \leq \lambda_n^c \mathbf{f}_n^k(t_n) + \lambda_n^c \tau_n \mathbf{g}_n^k(\tau_n). \quad (25)$$

Next we prove that the right-hand side times $e^{t_n} = \lambda_n^c$ vanishes. First, we have

$$\lambda_n^{2c} \mathbf{f}_n^k(t_n) \Rightarrow 0 \quad \text{as } n \rightarrow \infty \quad \text{for all } k \in \{1, 2\} \quad (26)$$

by Proposition 2 of Section 7 and Lemma 7 of Appendix C; the proposition holds because $4c < 1$ yields $(\lambda_n^{4c} \log \lambda_n) / n \rightarrow 0$ as $n \rightarrow \infty$. Second, $\boldsymbol{\sigma}_n(t) \in \Sigma_n(\zeta, \xi_n)$ if $t \in [0, \tau_n]$, and

$$\lim_{n \rightarrow \infty} \xi_n \lambda_n = \lim_{n \rightarrow \infty} \lambda_n^{1-d} = \infty \quad \text{and} \quad \lim_{n \rightarrow \infty} \frac{\lambda_n^{2c} t_n}{\xi_n \lambda_n} = \lim_{n \rightarrow \infty} c \lambda_n^{2c+d-1} \log \lambda_n = 0$$

since $d < 1 - 2c$. As a result, we may invoke Proposition 3 of Section 7 to obtain

$$\lambda_n^{2c} t_n \sup_{s \in [0, \tau_n]} \left| \mathcal{E}^k(\boldsymbol{\sigma}_n(s)) \right| \Rightarrow 0 \quad \text{as } n \rightarrow \infty \quad \text{for all } k \in \{1, 2\}.$$

Furthermore, $\mathbf{z}_n(t) \in \mathcal{A}(\zeta, \xi_n)$ for all $t \in [0, \tau_n]$, so we conclude from (10) and (21) that

$$\lambda_n^{2c} t_n \mathbf{g}_n^k(\tau_n) \Rightarrow 0 \quad \text{as } n \rightarrow \infty \quad \text{for all } k \in \{1, 2\}. \quad (27)$$

It follows from (25), (26) and (27) that

$$e^{t_n} \max_{k=1,2} \sup_{t \in [0, \tau_n]} \mathbf{d}_n^k(t) \leq \sum_{k=1,2} \left[\lambda_n^{2c} \mathbf{f}_n^k(t_n) + \lambda_n^{2c} t_n \mathbf{g}_n^k(\tau_n) \right] \Rightarrow 0 \quad \text{as } n \rightarrow \infty.$$

Since $\xi_n e^{t_n} = \lambda_n^{c-d}$ and $d > c$, we conclude that (24) holds, which proves (11). Note that the maximum on the left-hand side of (11) is bounded and thus uniformly integrable over n . Hence, the limit in (11) holds in expectation as well, which proves Theorem 2.

7 Approximation errors

In this section we establish some of the intermediate results that we used in the proofs of Theorems 1 and 2. In particular, we bound the last two terms on the right-hand side of (14). The following proposition takes care of the first of these error terms.

Proposition 2. *Consider sequences $\gamma_n, t_n > 0$ such that $\gamma_n^2 t_n / n \rightarrow 0$ as $n \rightarrow \infty$. Then*

$$\sup_{t \in [0, t_n]} \frac{\gamma_n}{V_n^k} |\mathcal{M}_n^k(t)| \Rightarrow 0 \quad \text{as } n \rightarrow \infty \quad \text{for all } k \in \{1, 2\}. \quad (28)$$

If $\gamma_n / \sqrt{n} \rightarrow 0$ as $n \rightarrow \infty$, then we further have

$$\gamma_n \left(\frac{\mathcal{M}_n^1}{V_n^1}, \frac{\mathcal{M}_n^2}{V_n^2} \right) \Rightarrow 0 \quad \text{in } D_{\mathbb{R}^2}[0, \infty) \quad \text{as } n \rightarrow \infty. \quad (29)$$

Proof. Let \mathcal{N} be a Poisson process with unit rate. By Doob's submartingale inequality,

$$P \left(\sup_{t \in [0, t_n]} \gamma_n \left| \frac{\mathcal{N}(nt)}{n} - t \right| \geq \varepsilon \right) \leq \left(\frac{\gamma_n}{\varepsilon n} \right)^2 E[|\mathcal{N}(nt_n) - nt_n|^2] = \left(\frac{\gamma_n}{\varepsilon} \right)^2 \frac{t_n}{n}. \quad (30)$$

Consider the processes defined as

$$\mathbf{i}_n^{k,s}(t) := \int_0^t \sum_{u \in \mathcal{J}_s^k(\boldsymbol{\sigma}_n(\tau))} r(\beta_n \Delta_n(\boldsymbol{\sigma}_n(\tau), u)) d\tau \leq V_n^k t \quad \text{for all } t \geq 0.$$

Since $V_n^k / n \rightarrow v^k$ as $n \rightarrow \infty$, there exists $c^k > 0$ such that $V_n^k \leq c^k n$ for all $n \geq 1$. Thus,

$$\begin{aligned} \sup_{t \in [0, t_n]} \frac{\gamma_n}{V_n^k} |\mathcal{M}_n^k(t)| &\leq \sup_{t \in [0, t_n]} \frac{\gamma_n}{V_n^k} |\mathcal{N}_+^k(\mathbf{i}_n^{k,-}(t)) - \mathbf{i}_n^{k,-}(t)| + \sup_{t \in [0, t_n]} \frac{\gamma_n}{V_n^k} |\mathcal{N}_-^k(\mathbf{i}_n^{k,+}(t)) - \mathbf{i}_n^{k,+}(t)| \\ &\leq \sup_{t \in [0, c^k t_n]} \frac{n \gamma_n}{V_n^k} \left| \frac{\mathcal{N}_+^k(nt)}{n} - t \right| + \sup_{t \in [0, c^k t_n]} \frac{n \gamma_n}{V_n^k} \left| \frac{\mathcal{N}_-^k(nt)}{n} - t \right|. \end{aligned}$$

It follows from (30) that (28) holds.

If $\gamma_n / \sqrt{n} \rightarrow 0$ as $n \rightarrow \infty$, then (28) implies that

$$\sup_{t \in [0, T]} \frac{\gamma_n}{V_n^k} |\mathcal{M}_n^k(t)| \Rightarrow 0 \quad \text{as } n \rightarrow \infty \quad \text{for all } T \geq 0 \quad \text{and } k \in \{1, 2\}.$$

We obtain (29) as a straightforward consequence of this observation. \square

For each configuration $\sigma \in \Sigma_n$, recall that

$$\mathcal{E}^k(\sigma) := \frac{2}{V_n^k} \sum_{u \in \mathcal{V}_n^k} \left[r(\beta_n \Delta_n(\sigma, u)) - r(2\beta_n \lambda_n \sigma(u) \mathcal{L}^k(z(\sigma))) \right].$$

Given two constants $\xi \in (0, 1)$ and $\zeta > 0$, we also recall that:

$$\begin{aligned} \mathcal{A}(\zeta, \xi) &:= \{z \in [-1 + \xi, 1 - \xi]^2 : \min\{\mathcal{L}^1(z), -\mathcal{L}^2(z)\} \geq \zeta\}, \\ \Sigma_n(\zeta, \xi) &:= \{\sigma \in \Sigma_n : z(\sigma) \in \mathcal{A}(\zeta, \xi)\}. \end{aligned}$$

The next proposition is used in the proofs of Theorems 1 and 2 to bound the last term on the right-hand side of (14). Its proof uses two lemmas that we derive in Appendix B.

Proposition 3. *Consider sequences $\gamma_n > 0$ and $\xi_n \in (0, 1)$ such that*

$$\lim_{n \rightarrow \infty} \xi_n \lambda_n = \infty \quad \text{and} \quad \lim_{n \rightarrow \infty} \frac{\gamma_n}{\xi_n \lambda_n} = 0. \quad (31)$$

Then the following limits hold:

$$\max_{\sigma \in \Sigma_n(\zeta, \xi_n)} \gamma_n \mathcal{E}^k(\sigma) \Rightarrow 0 \quad \text{as } n \rightarrow \infty \quad \text{for all } \zeta > 0 \quad \text{and } k \in \{1, 2\}.$$

Proof. Recall the notation $\bar{k} := 3 - k$. It follows from (13) and $|z_k| \leq 1$ that

$$\begin{aligned} \left| \Delta_n(\sigma, u) - 2\lambda_n \sigma(u) \mathcal{L}^k(z(\sigma)) \right| &\leq 2 \left| \sum_{v \in \mathcal{N}_n(u)} \sigma(v) - \lambda_n \left[a v^k z^k(\sigma) + b v^{\bar{k}} z^{\bar{k}}(\sigma) \right] \right| \\ &\quad + 2\alpha \lambda_n \left(\left| \frac{V_n^k}{n} - v^k \right| + \left| \frac{V_n^{\bar{k}}}{n} - v^{\bar{k}} \right| \right) + 2\alpha_n. \end{aligned} \quad (32)$$

Below we show that the right-hand side is small for most nodes $u \in \mathcal{V}_n^k$ when $\sigma \in \Sigma_n(\zeta, \xi_n)$ and n is sufficiently large. We will conclude that $\Delta_n(\sigma, u)$ and $2\lambda_n \sigma(u) \mathcal{L}^k(z(\sigma))$ have the same sign and then prove the proposition by leveraging the following inequality:

$$|r(\beta_n x) - r(\beta_n y)| \leq e^{-\beta_n \min\{|x|, |y|\}} \quad \text{if } \text{sign}(x) = \text{sign}(y). \quad (33)$$

This inequality holds with zero on the right-hand side if $\beta_n = \infty$ and we use (4).

Fix $\zeta > 0$ and $k \in \{1, 2\}$. Then choose some $0 < 2c < \zeta$, $d > 0$ and $n_0 \geq 1$ such that

$$\left| \frac{V_n^k}{n} - v^k \right| + \left| \frac{V_n^{\bar{k}}}{n} - v^{\bar{k}} \right| \leq \frac{c}{\max\{\alpha, a\}} \quad \text{and} \quad 3\sqrt{\frac{a V_n^k}{n}} + 2\sqrt{\frac{b V_n^{\bar{k}}}{n}} \leq d \quad \text{for all } n \geq n_0.$$

In addition, choose constants $\delta_n > 0$ satisfying the following conditions:

$$\lim_{n \rightarrow \infty} \delta_n = \infty, \quad \lim_{n \rightarrow \infty} \frac{\delta_n}{\xi_n \lambda_n} = 0 \quad \text{and} \quad \lim_{n \rightarrow \infty} \frac{\delta_n}{\gamma_n} = \infty. \quad (34)$$

If $\sqrt{\xi_n \lambda_n \gamma_n} \rightarrow \infty$ as $n \rightarrow \infty$, then take $\delta_n = \sqrt{\xi_n \lambda_n \gamma_n}$. Otherwise, $\gamma_n \rightarrow 0$ as $n \rightarrow \infty$, possibly only along some subsequence. If $\gamma_n \rightarrow 0$ as $n \rightarrow \infty$, then the third condition is implied by the first one and we can easily choose a sequence δ_n that satisfies the first two conditions. Now for each $\sigma \in \Sigma_n$ and $u \in \mathcal{V}_n^k$, define

$$A_n^k(u) := \left\{ \left| N_n^k(u) - a_n V_n^k \right| \geq \sqrt{a_n V_n^k \delta_n} \right\},$$

$$B_s^{k,l}(\sigma, u) := \left\{ \left| \hat{Y}_s^l(\sigma, u) - p_n(k, l) Y_s^l(\sigma) \right| \geq \sqrt{p_n(k, l) Y_s^l(\sigma) \delta_n} \right\}.$$

Moreover, consider the event defined as

$$C_s^k(\sigma, u) := A_n^k(u) \bigcup \left[\bigcup_{(l,t) \neq (k,s)} B_t^{k,l}(\sigma, u) \right] \quad \text{for all } \sigma \in \Sigma_n \quad \text{and} \quad u \in \mathcal{Y}_s^k(\sigma).$$

Lemmas 5 and 6 of Appendix B bound the probabilities of $A_n^k(u)$ and $B_t^{k,l}(\sigma, u)$. In the latter case, the bound only holds when $(l, t) \neq (k, s)$ since it relies on the sets $\hat{Y}_t^l(\sigma, u)$ being independent over $u \in \mathcal{Y}_s^k(\sigma)$. However, we can control the sets $\hat{Y}_s^k(\sigma, u)$ by considering the event $A_n^k(u)$ in combination with the events $B_t^{k,l}(\sigma, u)$, as done below.

Suppose that $\sigma \in \Sigma_n$ and $u \in \mathcal{Y}_s^k(\sigma)$. If we let $\bar{s} := -s$, then

$$\begin{aligned} \sum_{v \in \mathcal{N}_n(u)} \sigma(v) &= \hat{Y}_+^k(\sigma, u) - \hat{Y}_-^k(\sigma, u) + \hat{Y}_+^{\bar{k}}(\sigma, u) - \hat{Y}_-^{\bar{k}}(\sigma, u) \\ &= s \left[\hat{Y}_+^k(\sigma, u) + \hat{Y}_-^k(\sigma, u) \right] - 2s \hat{Y}_{\bar{s}}^k(\sigma, u) + \hat{Y}_+^{\bar{k}}(\sigma, u) - \hat{Y}_-^{\bar{k}}(\sigma, u) \\ &= s N_n^k(u) - 2s \hat{Y}_{\bar{s}}^k(\sigma, u) + \hat{Y}_+^{\bar{k}}(\sigma, u) - \hat{Y}_-^{\bar{k}}(\sigma, u). \end{aligned}$$

Similarly, we have $Y_+^k(\sigma) - Y_-^k(\sigma) = s V_n^k - 2s Y_{\bar{s}}^k(\sigma)$. Therefore, it follows from the above identity that $n \geq n_0$ and $[C_s^k(\sigma, u)]^c$ imply that

$$\begin{aligned} \left| \sum_{v \in \mathcal{N}_n(u)} \sigma(v) - \sum_{l=1,2} p_n(k, l) \left[Y_+^l(\sigma) - Y_-^l(\sigma) \right] \right| &\leq \left| N_n^k(u) - a_n V_n^k \right| + 2 \left| \hat{Y}_{\bar{s}}^k(\sigma, u) - a_n Y_{\bar{s}}^k(\sigma) \right| \\ &\quad + \left| \hat{Y}_+^{\bar{k}}(\sigma, u) - b_n Y_+^{\bar{k}}(\sigma) \right| + \left| \hat{Y}_-^{\bar{k}}(\sigma, u) - b_n Y_-^{\bar{k}}(\sigma) \right| \\ &\leq d \sqrt{\lambda_n \delta_n}, \end{aligned}$$

where the last inequality follows from the definition of $C_s^k(\sigma, u)$ and the observation that $Y_t^l(\sigma) \leq V_n^l$. Also, it is easy to check that the second term on the left-hand side is at most

at distance $c\lambda_n$ from $\lambda_n \left[av^k z^k(\sigma) + bv^{\bar{k}} z^{\bar{k}}(\sigma) \right]$. Thus, $n \geq n_0$ and $\left[C_s^k(\sigma, u) \right]^c$ imply that

$$\left| \sum_{v \in \mathcal{N}_n(u)} \sigma(v) - \lambda_n \left[av^k z^k(\sigma) + bv^{\bar{k}} z^{\bar{k}}(\sigma) \right] \right| \leq c\lambda_n + d\sqrt{\lambda_n \delta_n}.$$

Let us fix $n_1 \geq n_0$ such that

$$\psi_n := 2c\lambda_n + d\sqrt{\lambda_n \delta_n} + \alpha_n < \zeta\lambda_n \quad \text{for all } n \geq n_1.$$

If $\sigma \in \Sigma_n(\zeta, \xi_n)$, then $|\mathcal{L}^k(z(\sigma))| \geq \zeta$. Hence, by (32), $\Delta_n(\sigma, u)$ and $2\lambda_n \sigma(u) \mathcal{L}^k(z(\sigma))$ have the same sign if $C_s^k(\sigma, u)$ does not hold, $u \in \mathcal{Y}_s^k(\sigma)$ and $n \geq n_1$. Then (33) yields

$$\left| r(\beta_n \Delta_n(\sigma, u)) - r(2\beta_n \lambda_n \sigma(u) \mathcal{L}^k(z(\sigma))) \right| \leq e^{-2\beta_n(\zeta\lambda_n - \psi_n)} + \mathbb{1}_{\{C_s^k(\sigma, u)\}}$$

for all $\sigma \in \Sigma_n(\zeta, \xi_n)$, $u \in \mathcal{Y}_s^k(\sigma)$ and $n \geq n_1$. Thus, $\sigma \in \Sigma_n(\zeta, \xi_n)$ and $n \geq n_1$ imply that

$$\begin{aligned} \gamma_n \mathcal{E}^k(\sigma) &\leq 2\gamma_n e^{-2\beta_n(\zeta\lambda_n - \psi_n)} + \frac{2\gamma_n}{V_n^k} \sum_{s=-1,1} \sum_{u \in \mathcal{Y}_s^k(\sigma)} \mathbb{1}_{\{C_s^k(\sigma, u)\}} \\ &\leq 2\gamma_n e^{-2\beta_n(\zeta\lambda_n - \psi_n)} + \frac{2\gamma_n}{V_n^k} \sum_{u \in \mathcal{V}_n^k} \mathbb{1}_{\{A_n^k(u)\}} + \frac{2\gamma_n}{V_n^k} \sum_{s=-1,1} \sum_{(l,t) \neq (k,s)} \sum_{u \in \mathcal{Y}_s^k(\sigma)} \mathbb{1}_{\{B_t^{k,l}(\sigma, u)\}}. \end{aligned}$$

It follows from $2c < \zeta$ and (34) that the first term on the right vanishes as $n \rightarrow \infty$. The proof is completed by invoking Lemmas 5 and 6 from Appendix B, which hold by (34) and imply that the last two terms on the right-hand side converge weakly to zero as $n \rightarrow \infty$. \square

8 Numerical experiments

In this section we present and discuss the results of several numerical experiments.¹ First we evaluate the impact of the hyperparameters α and β_n on the classification error of Algorithm 1. Then we compare this algorithm with several other algorithms.

8.1 Parameter selection

Table 1 shows the mean relative classification error of Algorithm 1 in logarithmic-degree regimes for different values of α and β_n ; for the experiments here and below the parameters of the graph are given in the table captions. The relative errors that we observed were roughly 0%, 42.9%, 57.1% and 100% in a few experiments; the second and third values correspond to the monochromatic outcomes while the last value corresponds to labeling each node with the opposite community. The averages shown in Table 1 depend on how many times each of the above relative errors was observed over all the experiments.

¹Code available at https://github.com/diegogolds/ising_clustering.

η	$a = 7 \text{ and } b = 1$								$a = 10 \text{ and } b = 1$							
	$\alpha = 0$				$\alpha = 6$				$\alpha = 0$				$\alpha = 6$			
	$\beta_n = 1$		$\beta_n = \infty$		$\beta_n = 1$		$\beta_n = \infty$		$\beta_n = 1$		$\beta_n = \infty$		$\beta_n = 1$		$\beta_n = \infty$	
	μ	σ	μ	σ	μ	σ	μ	σ	μ	σ	μ	σ	μ	σ	μ	σ
0.01	31.4	21.0	32.9	22.2	10.0	30.0	10.0	30.0	21.4	26.5	21.1	22.5	30.0	45.8	10.0	30.0
0.02	25.7	21.0	37.1	19.4	0.00	0.00	0.00	0.00	8.57	17.1	12.9	19.6	0.00	0.00	0.00	0.00
0.03	25.7	21.0	25.7	21.0	0.00	0.00	0.00	0.00	4.29	12.9	8.57	17.1	0.00	0.00	0.00	0.00
0.04	18.6	23.1	17.1	21.0	0.00	0.00	0.00	0.00	0.00	0.00	4.29	12.9	0.00	0.00	0.00	0.00
0.05	17.1	21.0	17.1	21.0	0.00	0.00	0.00	0.00	0.00	0.00	0.00	0.00	0.00	0.00	0.00	0.00
0.06	4.29	12.9	8.57	17.1	0.00	0.00	0.00	0.00	0.00	0.00	0.00	0.00	0.00	0.00	0.00	0.00
0.07	0.00	0.00	0.00	0.00	0.00	0.00	0.00	0.00	0.00	0.00	0.00	0.00	0.00	0.00	0.00	0.00
0.08	0.00	0.00	0.00	0.00	0.00	0.00	0.00	0.00	0.00	0.00	0.00	0.00	0.00	0.00	0.00	0.00
0.09	0.00	0.00	0.00	0.00	0.00	0.00	0.00	0.00	0.00	0.00	0.00	0.00	0.00	0.00	0.00	0.00
0.10	0.00	0.00	0.00	0.00	0.00	0.00	0.00	0.00	0.00	0.00	0.00	0.00	0.00	0.00	0.00	0.00

Table 1: Percentual classification error when $V_n^1 = 10000$, $V_n^2 = 7500$ and $n = 10000$. The headers μ and σ refer to the mean and standard deviation over 10 experiments, respectively. In all the experiments Algorithm 1 is ran for at most 5×10^4 spin flips in total; when $\beta_n = \infty$ the algorithm may stop sooner.

We observe that the algorithm performs much better for $\alpha = 6$ than $\alpha = 0$. In particular, the mean relative error with $\alpha = 6$ is negligible for all $\eta \geq 0.02$, whereas the algorithm struggles with small values of η when $\alpha = 0$, especially in the more challenging regime with $a = 7$. The value of β_n does not affect the mean relative error significantly. However, it makes the algorithm stop in fewer iterations because eventually the flip rate of every spin is equal to zero. The average number of iterations observed when $\beta_n = \infty$ ranges roughly between 8.3×10^3 and 1.2×10^4 iterations across all regimes considered, which is significantly less than the 5×10^4 iterations in the cases where $\beta_n = 1$.

The effect of the hyperparameter α on performance can be understood intuitively by considering the mean-field approximation in (15). The dynamics of \mathbf{z}_n are mostly governed by the terms $\tanh(\beta_n \lambda_n \mathcal{L}^k(\mathbf{z}_n))$, which can be approximated by $\text{sign}(\mathcal{L}^k(\mathbf{z}_n))$ when $\beta_n \lambda_n$ is large. The latter terms drive \mathbf{z}_n in the direction indicated by the diagrams of Figure 3. If α satisfies (5), then this direction points to $(1, -1)$ in a half-cone that contains $(\eta, -\eta)$, but \mathbf{z}_n is driven towards $(1, 1)$ or $(-1, -1)$ in the adjacent regions if $\alpha < (a+b)/2$. The random error terms in (15) can push \mathbf{z}_n outside the half-cone where the mean-field drift points in the right direction, particularly if η is small. Nevertheless, the mean-field drift points into the half-cone near its boundary when $\alpha > (a+b)/2$. Therefore, setting $\alpha > (a+b)/2$ makes the algorithm more robust against the random error terms in (15) and results in small classification errors for a broader range of values of η . Observe that, in practice, α can be selected so that $\alpha > (a+b)/2$ using Remark 2.

8.2 Performance evaluation

Table 2 compares the performance of Algorithm 1 with that of several semi-supervised clustering algorithms discussed in Section 1, which we briefly describe below.

- *Asynchronous and Synchronous Consensus Dynamics.* The algorithm is initialized

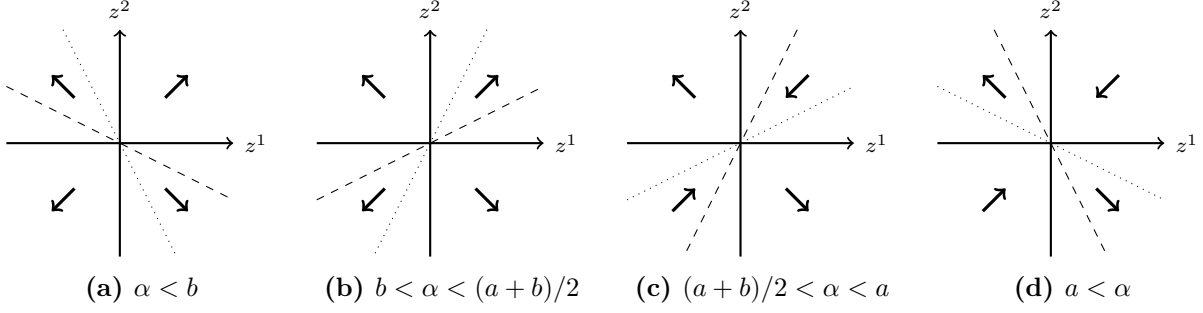


Figure 3: The arrows show the direction of the vector $(\text{sign}(\mathcal{L}^1(z)), \text{sign}(\mathcal{L}^2(z)))$ when (5) holds. The dotted and dashed lines are $\mathcal{L}^1(z) = 0$ and $\mathcal{L}^2(z) = 0$, respectively.

by assigning values -1 and 1 to the nodes with revealed community labels, according to their respective labels, whereas the initial value is 0 for all the other nodes. The nodes with unknown community labels replace their value iteratively by the average value across the neighboring nodes, and after multiple iterations, the community labels are estimated by looking at the sign of the value associated with each node. In the asynchronous version, the node that updates its value is selected uniformly at random, whereas all nodes are updated simultaneously in the synchronous version.

- *Gossiping Algorithm.* The algorithm is initialized as above. On each iteration, an edge is selected uniformly at random and the average of the values in the endpoints of the edge is computed. If the community of a node in one endpoint of the edge was not revealed at the beginning of the algorithm, then the value of the node is replaced by the average mentioned earlier. After multiple iterations of the algorithm, the community labels are estimated using the signs of the values assigned to the nodes. As noted in Section 1, this algorithm has been analyzed in [49].
- *Generalized Laplacian Methods.* Let $X(t)$ and Y be $V_n \times 2$ matrices, such that $X(0)$ is full of zeros and the entries of Y are zeros and ones indicating the communities of the nodes with revealed labels. On each iteration, these algorithms perform the update $X(t+1) = \gamma D^{-\delta} A D^{\delta-1} X(t) + (1-\gamma)Y$, where A is the adjacency matrix and D is the diagonal matrix of degrees. In our experiments we set $\gamma = 0.95$ and $\delta \in \{0, 0.5, 1\}$, which correspond to PageRank, the Normalized Laplacian and the Standard Laplacian Methods, respectively. In [5] these methods are shown to solve a suitable regularized optimization problem and have probabilistic interpretation in terms of random walks. After several iterations, the community labels are estimated by looking at the maximum value on each row of $X(t)$.
- *Poisson Learning.* The algorithm solves a Poisson equation that involves the graph Laplacian and has a right-hand side defined using the revealed community labels. The solution of the equation is estimated through an iterative procedure similar to that described above; see [12, Algorithm 1] for details.

	η	0.01	0.02	0.03	0.04	0.05	0.06	0.07	0.08	0.09	0.10
Algorithm 1	μ	10.1	0.14	0.11	0.13	0.11	0.12	0.12	0.12	0.12	0.12
	σ	29.9	0.03	0.03	0.05	0.03	0.04	0.04	0.02	0.03	0.04
Asynchronous Consensus	μ	15.8	12.6	12.7	11.3	10.0	8.18	6.91	5.77	4.95	4.42
	σ	4.54	1.23	0.85	0.19	0.81	0.31	0.28	0.20	0.35	0.32
Synchronous Consensus	μ	15.8	12.6	12.7	11.3	10.1	8.18	6.91	5.77	4.95	4.42
	σ	4.40	1.26	0.83	0.19	0.82	0.32	0.29	0.20	0.36	0.32
Gossiping Algorithm	μ	44.4	39.5	36.4	34.6	33.5	32.0	30.9	29.9	29.1	28.6
	σ	1.84	1.69	0.69	0.57	0.64	0.32	0.72	0.42	0.46	0.86
Standard Laplacian	μ	13.0	12.6	12.9	12.1	10.4	8.98	7.52	6.35	5.48	4.88
	σ	2.16	1.22	1.15	0.41	0.40	0.30	0.25	0.34	0.29	0.24
Normalized Laplacian	μ	12.2	12.1	12.3	12.0	10.4	8.91	7.52	6.33	5.47	4.75
	σ	0.62	0.38	0.49	0.34	0.43	0.25	0.23	0.30	0.27	0.12
PageRank Method	μ	12.1	12.4	12.3	12.0	10.4	8.92	7.59	6.46	5.57	4.79
	σ	0.47	0.34	0.37	0.29	0.45	0.27	0.24	0.30	0.24	0.17
Poisson Learning	μ	11.6	12.0	11.9	11.4	9.58	8.10	6.85	5.74	4.93	4.26
	σ	0.44	0.32	0.39	0.28	0.44	0.24	0.26	0.28	0.22	0.15

Table 2: Percentual relative errors for $V_n^1 = V_n^2 = n = 5000$, $\lambda_n = \log n$, $a = 3$ and $b = 1$. The headers μ and σ refer to the mean and standard deviation over 10 experiments, respectively. For Algorithm 1, the hyperparameters are $\alpha = 10$ and $\beta_n = \infty$.

For each row of Table 2, we ran all algorithms 10 times using the same graph for all algorithms on each run. Each algorithm was ran for a number of iterations such that each node could be updated 20 times on average. For Algorithm 1 and the Asynchronous Consensus Dynamics, the maximum number of iterations was $20V_n = 2 \times 10^5$ since a single node is updated on each iteration. However, Algorithm 1 typically stopped much sooner, with the average number of spin flips ranging between 6548 for $\eta = 0.1$ and 10445 for $\eta = 0.01$, i.e., 0.65 and 1.04 flips per node, respectively. For the Synchronous Consensus Dynamics, the Generalized Laplacian Methods and Poisson Learning, we set the number of iterations to 20 since all nodes are updated on each iteration. For Gossiping, the number of iterations was $20(a+b)V_n\lambda_n/2 \simeq 3.4 \times 10^6$, since each node needs as many iterations as its degree to be paired with each neighbor and two nodes are updated on each iteration.

Algorithm 1 performed much better than the other algorithms, especially for $\eta \geq 0.02$, where its mean relative error is almost zero. For $\eta = 0.01$, the relative error of this algorithm was nearly zero in all the experiments except one, where it returned opposite community labels for nearly all the nodes; this explains the high standard deviation in this case. Except for the Gossiping Algorithm, which had by far the worst performance, the other algorithms had very similar mean relative errors for all values of $\eta \geq 0.02$, which in the best case were more than 4% above the mean relative error obtained by Algorithm 1.

9 Conclusion and open problems

We have proposed Algorithm 1 for learning the community labels of a graph with two communities when the edges of the graph are known and a small fraction of the community

labels are disclosed in advance. This algorithm is based on the Glauber dynamics for an Ising model where the energy function includes a quadratic penalty on the magnetization of the entire graph, and it subsumes the Label Propagation algorithm. In particular, our results cover the Label Propagation algorithm when the inverse temperature is infinite and the quadratic penalty is omitted by setting the hyperparameter $\alpha = 0$.

We have analyzed Algorithm 1 in the SBM with slowly diverging mean degree, deriving a mean-field limit that describes how the algorithm updates the community labels over time. In practice, this result can be used to estimate how long the algorithm should run to achieve a target accuracy level. We have further shown that almost exact recovery can be achieved in a number of updates that is quasi-linear in the number of nodes. In the special case of Label Propagation, rigorous results of this kind had only been obtained in a substantially less challenging SBM regime, suitably dense with a rather sparse cut.

The above results establish that Algorithm 1 can perform the clustering task efficiently, and have been confirmed by our numerical experiments, which show that often less than one update per node is enough to achieve a negligible classification error. Furthermore, these numerical results show that Algorithm 1 outperforms multiple semi-supervised clustering algorithms with similar complexity in a challenging logarithmic-degree regime.

We would like to conclude by mentioning a couple of open problems that seem relevant from a practical perspective and at the same time mathematically challenging.

1. Our theoretical results prove that Algorithm 1 is asymptotically effective provided that the hyperparameter α lies in the interval given by (5). However, our numerical results show that, for graphs of a given size, performance improves if α is selected within a suitable subinterval, as explained in Figure 3. Characterizing this behavior rigorously seems difficult and may require a nonasymptotic approach, different from the one adopted in the present paper.
2. Our numerical results suggest that Algorithm 1 could be effective in the unsupervised case as well, i.e., if it is initialized by sampling all the spins uniformly at random. In this case $\mathbf{z}_n(0)$ vanishes as $n \rightarrow \infty$, but our simulations show that \mathbf{z}_n moves away from zero after some short fluctuations and then continues moving towards a state where the communities have opposite magnetizations. Proving this rigorously seems challenging and may require rescaling \mathbf{z}_n depending on how close it is to zero at the current time, with the behavior near zero being more similar to a diffusion.

Appendix A Tightness result

In this section we prove Lemma 1, which requires the following standard result.

Lemma 3. *Let $\|\cdot\|$ be a norm on \mathbb{R}^2 . For each $T \geq 0$ and $h > 0$, we define the local modulus of continuity of a function $\mathbf{x} \in D_{\mathbb{R}^2}[0, \infty)$ as*

$$w_T(\mathbf{x}, h) := \sup \{ \|\mathbf{x}(t) - \mathbf{x}(s)\| : s, t \in [0, T] \text{ and } |t - s| \leq h \}.$$

Consider a sequence of processes $\{\mathbf{x}_n : n \geq 1\}$ with sample paths in $D_{\mathbb{R}^2}[0, \infty)$ such that:

- (a) $\mathbf{x}_n(t)$ is tight in \mathbb{R}^2 for all t in some dense subset of $[0, \infty)$,
- (b) for all $T \geq 0$, we have

$$\lim_{h \rightarrow 0} \limsup_{n \rightarrow \infty} E [\min \{w_T(\mathbf{x}_n, h), 1\}] = 0.$$

Then $\{\mathbf{x}_n : n \geq 1\}$ is tight in $D_{\mathbb{R}^2}[0, \infty)$ with respect to the topology of uniform convergence over compact sets. Also, every subsequence of $\{\mathbf{x}_n : n \geq 1\}$ has a further subsequence that converges weakly in $D_{\mathbb{R}^2}[0, \infty)$ to a process that is continuous with probability one.

Proof. For each $T \geq 0$ and $h > 0$, the modified modulus of continuity is defined as

$$\tilde{w}_T(\mathbf{x}, h) := \inf_{\mathcal{I}} \max_{I \in \mathcal{I}} \sup_{s, t \in I} \|\mathbf{x}(t) - \mathbf{x}(s)\| \quad \text{for all } \mathbf{x} \in D_{\mathbb{R}^2}[0, \infty),$$

where the infimum extends over all partitions \mathcal{I} of $[0, T]$ into subintervals $I = [s, t)$ such that $t - s \geq h$ if $t < T$. We observe that

$$\tilde{w}_T(\mathbf{x}, h) \leq w_T(\mathbf{x}, h) \quad \text{for all } \mathbf{x} \in D_{\mathbb{R}^2}[0, \infty), \quad T \geq 0 \quad \text{and} \quad h > 0.$$

It follows from [27, Theorems 23.8 and 23.9] that $\{\mathbf{x}_n : n \geq 1\}$ is tight in $D_{\mathbb{R}^2}[0, \infty)$ if (a) and (b) hold. By Prohorov's theorem, every subsequence of $\{\mathbf{x}_n : n \geq 1\}$ has a further subsequence that converges weakly in $D_{\mathbb{R}^2}[0, \infty)$, and [27, Theorem 23.9] implies that the limiting process is almost surely continuous. \square

We are now ready to prove Lemma 1.

Proof of Lemma 1. It is clear that (a) of Lemma 3 holds automatically because \mathbf{z}_n takes values in the compact set $[-1, 1]^2$. Hence, it suffices to check that (b) holds as well.

Note that the jump times of \mathbf{z}_n can be obtained from a thinning of a Poisson process \mathcal{N}_n with rate V_n since the spins flip at rate less than one. Recall that $V_n^k/n \rightarrow v^k$ as $n \rightarrow \infty$. Thus, there exists $c > 0$ such that $V_n^k \geq cn$ for all $k \in \{1, 2\}$ and $n \geq 1$, and we have

$$\left\| \mathbf{z}_n(t) - \mathbf{z}_n(t^-) \right\|_1 = \left| \mathbf{z}_n^k(t) - \mathbf{z}_n^k(t^-) \right| = \frac{2}{V_n^k} \leq \frac{2}{cn}$$

whenever the spin of a node in community V_n^k flips at time t . If we consider the modulus of continuity defined by the norm $\|\cdot\|_1$, then we obtain

$$\begin{aligned} E[w_T(\mathbf{z}_n, h)] &\leq 2E \left[\sup_{t \in [0, T]} \left| \frac{\mathcal{N}_n(t+h) - \mathcal{N}_n(t)}{cn} \right| \right] \\ &\leq 2E \left[\sup_{t \in [0, T]} \left| \frac{\mathcal{N}_n(t+h) - V_n(t+h)}{cn} \right| \right] + 2E \left[\sup_{t \in [0, T]} \left| \frac{\mathcal{N}_n(t) - V_n(t)}{cn} \right| \right] + \frac{2hV_n}{cn}. \end{aligned}$$

By Doob's submartingale inequality moment version,

$$E \left[\sup_{t \in [0, T]} \left| \frac{\mathcal{N}_n(t) - V_n(t)}{cn} \right|^2 \right] \leq \frac{4V_n T}{c^2 n^2}.$$

Then it follows from Jensen's inequality that

$$E[w_T(\mathbf{z}_n, h)] \leq 2\sqrt{\frac{4V_n(T+h)}{c^2 n^2}} + 2\sqrt{\frac{4V_n T}{c^2 n^2}} + \frac{2hV_n}{cn}.$$

Note that $V_n/n \rightarrow v^1 + v^2$ as $n \rightarrow \infty$. Hence, we conclude that property (b) holds:

$$\lim_{h \rightarrow 0} \limsup_{n \rightarrow \infty} E[\min\{w_T(\mathbf{z}_n, 1), 1\}] \leq \lim_{h \rightarrow 0} \limsup_{n \rightarrow \infty} E[w_T(\mathbf{z}_n, h)] = 0,$$

and we complete the proof by invoking Lemma 3. \square

Appendix B Concentration inequalities

The following lemma contains some Chernoff bounds for the binomial distribution, which we will use to prove Lemmas 5 and 6 below.

Lemma 4. *If $X \sim \text{Bin}(n, p)$ is binomially distributed with mean $\mu := np$, then*

$$\begin{aligned} P(X \geq \mu + x) &\leq e^{-\mu\varphi(\frac{x}{\mu})} \quad \text{for all } x \geq 0, \\ P(|X - \mu| \geq x\mu) &\leq 2e^{-\frac{x^2\mu}{3}} \quad \text{for all } x \in (0, 3/2], \end{aligned}$$

where $\varphi(x) := (1+x)\log(1+x) - x$ for all $x \geq 0$.

Proof. The inequalities are proved in [26, Theorem 2.1 and Corollary 2.3], respectively. \square

The following lemma bounds the fraction of nodes $u \in \mathcal{V}_n^k$ such that the number of neighbors that u has in \mathcal{V}_n^k deviates too much from the expected value.

Lemma 5. *Given $\delta_n > 0$, recall that*

$$A_n^k(u) := \left\{ |N_n^k(u) - a_n V_n^k| \geq \sqrt{a_n V_n^k \delta_n} \right\} \quad \text{for all } u \in \mathcal{V}_n^k.$$

Suppose that the sequences $\gamma_n > 0$ and δ_n are such that

$$\lim_{n \rightarrow \infty} \delta_n = \infty, \quad \limsup_{n \rightarrow \infty} \frac{\delta_n}{\lambda_n} < \infty \quad \text{and} \quad \limsup_{n \rightarrow \infty} \frac{\gamma_n}{\delta_n} < \infty.$$

Then the following limit holds:

$$\frac{\gamma_n}{n} \sum_{u \in \mathcal{V}_n^k} \mathbb{1}_{\{A_n^k(u)\}} \Rightarrow 0 \quad \text{as } n \rightarrow \infty \quad \text{for all } k \in \{1, 2\}.$$

Proof. Given $\varepsilon > 0$, Markov's inequality yields

$$\begin{aligned} P\left(\frac{\gamma_n}{n} \sum_{u \in \mathcal{V}_n^k} \mathbb{1}_{\{A_n^k(u)\}} \geq \varepsilon\right) &\leq \left(\frac{\gamma_n}{\varepsilon n}\right)^2 E\left[\sum_{u, v \in \mathcal{V}_n^k} \mathbb{1}_{\{A_n^k(u)\}} \mathbb{1}_{\{A_n^k(v)\}}\right] \\ &= \left(\frac{\gamma_n}{\varepsilon n}\right)^2 \left[V_n^k P(A_n^k(u)) + V_n^k (V_n^k - 1) P(A_n^k(u) \cap A_n^k(v))\right], \end{aligned}$$

where the nodes u and v in the last line satisfy $u, v \in \mathcal{V}_n^k$ and $u \neq v$. Therefore, it suffices to prove that the right-hand side approaches zero as $n \rightarrow \infty$ for each $\varepsilon > 0$.

Since δ_n/λ_n is bounded, there exists $c \in (0, 1)$ such that

$$\sqrt{\frac{c\delta_n}{a_n(V_n^k - i)}} \in (0, 3/2] \quad \text{for all } i \in \{1, 2\} \quad \text{and all large enough } n.$$

Furthermore, let us consider all the intervals of the form

$$\left(a_n(V_n^k - i) + j - \sqrt{a_n(V_n^k - i)c\delta_n}, a_n(V_n^k - i) + j + \sqrt{a_n(V_n^k - i)c\delta_n}\right)$$

with $i \in \{1, 2\}$ and $j \in \{0, 1\}$. These intervals are contained in the interval

$$\left(a_n V_n^k - \sqrt{a_n V_n^k \delta_n}, a_n V_n^k + \sqrt{a_n V_n^k \delta_n}\right) \quad \text{for all large enough } n.$$

Using the above observations, we conclude from Lemma 4 that

$$P(A_n^k(u)) \leq P\left(|N_n^k(u) - a_n(V_n^k - 1)| \geq \sqrt{a_n(V_n^k - 1)c\delta_n}\right) \leq 2e^{-\frac{c\delta_n}{3}}$$

for all sufficiently large n , because $N_n^k(u) \sim \text{Bin}(V_n^k - 1, a_n)$.

In addition, we observe that

$$\begin{aligned} P(A_n^k(u) \cap A_n^k(v)) &= P(A_n^k(u) \cap A_n^k(v) \mid u \not\sim v)(1 - a_n) + P(A_n^k(u) \cap A_n^k(v) \mid u \sim v)a_n \\ &= \left[P(A_n^k(u) \mid u \not\sim v)\right]^2 (1 - a_n) + \left[P(A_n^k(u) \mid u \sim v)\right]^2 a_n. \end{aligned}$$

Applying Lemma 4 again, we obtain

$$\begin{aligned} P\left(A_n^k(u) \mid u \asymp v\right) &\leq P\left(\left|N_n^k(u) - a_n(V_n^k - 2)\right| \geq \sqrt{a_n(V_n^k - 2)c\delta_n} \mid u \asymp v\right) \leq 2e^{-\frac{c\delta_n}{3}}, \\ P\left(A_n^k(u) \mid u \sim v\right) &\leq P\left(\left|N_n^k(u) - 1 - a_n(V_n^k - 2)\right| \geq \sqrt{a_n(V_n^k - 2)c\delta_n} \mid u \sim v\right) \leq 2e^{-\frac{c\delta_n}{3}}, \end{aligned}$$

for all large enough n . In the former case, note that $N_n^k(u) \sim \text{Bin}(V_n^k - 2, a_n)$ when $u \asymp v$, whereas $N_n^k(u) - 1 \sim \text{Bin}(V_n^k - 2, a_n)$ in the latter case where $u \sim v$.

Putting the above inequalities together, we get

$$P\left(\frac{\gamma_n}{n} \sum_{u \in \mathcal{V}_n^k} \mathbb{1}_{\{A_n^k(u)\}} \geq \varepsilon\right) \leq \left(\frac{\gamma_n}{\varepsilon n}\right)^2 \left[2V_n^k e^{-\frac{c\delta_n}{3}} + 4V_n^k(V_n^k - 1)e^{-\frac{2c\delta_n}{3}}\right]$$

for all sufficiently large n . Because γ_n/δ_n is bounded and $\delta_n \rightarrow \infty$ as $n \rightarrow \infty$, we conclude that the right-hand side vanishes and thus complete the proof. \square

The next lemma is similar to Lemma 5 in spirit but takes into account the spin of the nodes.

Lemma 6. *Given $\delta_n > 0$, recall that*

$$B_s^{k,l}(\sigma, u) := \left\{ \left| \hat{Y}_s^l(\sigma, u) - p_n(k, l)Y_s^l(\sigma) \right| \geq \sqrt{p_n(k, l)Y_s^l(\sigma)\delta_n} \right\}$$

for all $\sigma \in \Sigma_n$ and $u \in \mathcal{V}_n^k$. Suppose that $\gamma_n, \delta_n > 0$ and $\xi_n \in (0, 1)$ are such that

$$\lim_{n \rightarrow \infty} \delta_n = \infty, \quad \lim_{n \rightarrow \infty} \frac{\delta_n}{\xi_n \lambda_n} = 0 \quad \text{and} \quad \lim_{n \rightarrow \infty} \frac{\delta_n}{\gamma_n} = \infty.$$

If we fix $\zeta > 0$ and $(k, s) \neq (l, t)$, then we have

$$\max_{\sigma \in \Sigma_n(\zeta, \xi_n)} \frac{\gamma_n}{n} \sum_{u \in \mathcal{Y}_s^k(\sigma)} \mathbb{1}_{\{B_t^{k,l}(\sigma, u)\}} \Rightarrow 0 \quad \text{as } n \rightarrow \infty.$$

Proof. If $\sigma \in \Sigma_n(\zeta, \xi_n)$, then $Y_t^l(\sigma) \geq \xi_n V_n^l/2$. Hence, for all sufficiently large n ,

$$0 < \sqrt{\frac{\delta_n}{p_n(k, l)Y_s^l(\sigma)}} \leq \sqrt{\frac{2\delta_n}{\xi_n p_n(k, l)V_n^l}} \leq \sqrt{\frac{2\delta_n n}{b\xi_n \lambda_n V_n^l}} \leq \frac{3}{2}.$$

Since $\hat{Y}_t^l(\sigma, u) \sim \text{Bin}(Y_t^l(\sigma), p_n(k, l))$ for all $u \in \mathcal{Y}_s^k(\sigma)$, Lemma 4 implies that

$$P\left(B_t^{k,l}(\sigma, u)\right) \leq 2e^{-\frac{\delta_n}{3}} \quad \text{for all } \sigma \in \Sigma_n(\zeta, \xi_n) \quad u \in \mathcal{Y}_s^k(\sigma) \quad \text{and all large enough } n.$$

Furthermore, the random variables $\{\hat{Y}_t^l(\sigma, u) : u \in \mathcal{Y}_s^k(\sigma)\}$ are independent if σ is fixed

since $(k, s) \neq (l, t)$. Thus, for all large enough n , the next stochastic inequality holds:

$$\sum_{u \in \mathcal{Y}_s^k(\sigma)} \mathbb{1}_{\{B_t^{k,l}(\sigma, u)\}} \leq_{st} \text{Bin}\left(Y_s^k(\sigma), 2e^{-\frac{\delta_n}{3}}\right) \quad \text{for all } \sigma \in \Sigma_n(\zeta, \xi_n).$$

Fix $\varepsilon > 0$ and let us write $\mu := 2Y_s^k(\sigma)e^{-\frac{\delta_n}{3}}$ and $x := \varepsilon n / \gamma_n - \mu$ for brevity. It follows from the above stochastic inequality and Lemma 4 that

$$P\left(\frac{\gamma_n}{n} \sum_{u \in \mathcal{Y}_s^k(\sigma)} \mathbb{1}_{\{B_t^{k,l}(\sigma, u)\}} \geq \varepsilon\right) \leq e^{-\mu\varphi\left(\frac{x}{\mu}\right)} \quad \text{for all } \sigma \in \Sigma_n(\zeta, \xi_n)$$

and all large enough n , where φ is defined as in the statement of Lemma 4. Now note that

$$\begin{aligned} \mu\varphi\left(\frac{x}{\mu}\right) &= \mu\varphi\left(\frac{\varepsilon n}{\mu\gamma_n} - 1\right) = \frac{\varepsilon n}{\gamma_n} \left[\log\left(\frac{\varepsilon n}{\mu\gamma_n}\right) - 1 \right] + \mu \\ &\geq \frac{\varepsilon n}{\gamma_n} \left[\log\left(\frac{\varepsilon n e^{\frac{\delta_n}{3}}}{2V_n^k \gamma_n}\right) - 1 \right] = \varepsilon n \left[\frac{\delta_n}{3\gamma_n} - \frac{1}{\gamma_n} \log\left(\frac{2V_n^k \gamma_n}{\varepsilon n}\right) - \frac{1}{\gamma_n} \right] \end{aligned}$$

for all $\sigma \in \Sigma_n(\zeta, \xi_n)$, where we used that $Y_s^k(\sigma) \leq V_n^k$. Hence, for all sufficiently large n ,

$$P\left(\max_{\sigma \in \Sigma_n(\zeta, \xi_n)} \frac{\gamma_n}{n} \sum_{u \in \mathcal{Y}_s^k(\sigma)} \mathbb{1}_{\{B_t^{k,l}(\sigma, u)\}} \geq \varepsilon\right) \leq 2^{V_n} e^{-\varepsilon n \left[\frac{\delta_n}{3\gamma_n} - \frac{1}{\gamma_n} \log\left(\frac{2V_n^k \gamma_n}{\varepsilon n}\right) - \frac{1}{\gamma_n} \right]},$$

and the right-hand side approaches zero as $n \rightarrow \infty$ because $\delta_n / \gamma_n \rightarrow \infty$. \square

Appendix C Other intermediate results

Proof of Proposition 1. Let A denote the adjacency matrix of \mathcal{G} . Then

$$p_{\mathcal{G}}(\sigma) = \prod_{u < v} \left[a_n^{A_{uv}} (1 - a_n)^{1-A_{uv}} \mathbb{1}_{\{\sigma(u)=\sigma(v)\}} + b_n^{A_{uv}} (1 - b_n)^{1-A_{uv}} \mathbb{1}_{\{\sigma(u) \neq \sigma(v)\}} \right], \quad (35)$$

where we have identified \mathcal{V}_n with $\{1, \dots, V_n\}$. It follows that

$$\begin{aligned} \log p_{\mathcal{G}}(\sigma) &= \sum_{u < v} [A_{uv} \log a_n + (1 - A_{uv}) \log(1 - a_n)] \mathbb{1}_{\{\sigma(u)=\sigma(v)\}} \\ &\quad + \sum_{u < v} [A_{uv} \log b_n + (1 - A_{uv}) \log(1 - b_n)] \mathbb{1}_{\{\sigma(u) \neq \sigma(v)\}} \\ &= \frac{1}{2} \sum_{u < v} \left[A_{uv} \log\left(\frac{a_n}{b_n}\right) + (1 - A_{uv}) \log\left(\frac{1 - a_n}{1 - b_n}\right) \right] \sigma(u) \sigma(v) \\ &\quad + \frac{1}{2} \sum_{u < v} [A_{uv} \log(a_n b_n) + (1 - A_{uv}) \log((1 - a_n)(1 - b_n))], \end{aligned} \quad (36)$$

where we used that $\mathbb{1}_{\{\sigma(u)=\sigma(v)\}} = [1 + \sigma(u)\sigma(v)]/2$ and $\mathbb{1}_{\{\sigma(u) \neq \sigma(v)\}} = [1 - \sigma(u)\sigma(v)]/2$.

Note that p_G and $\log p_G$ have the same maximizers. Moreover, the second term on the right-hand side of (36) does not depend on σ , so we may focus on maximizing the first term. This term is equal to

$$\frac{1}{2} \log \left(\frac{b_n(1-a_n)}{a_n(1-b_n)} \right) \left[- \sum_{u < v} A_{uv} \sigma(u) \sigma(v) + \rho_n \sum_{u < v} \sigma(u) \sigma(v) \right].$$

Furthermore, observe that

$$\sum_{u < v} A_{uv} \sigma(u) \sigma(v) = \frac{1}{2} \sum_{u \sim v} \sigma(u) \sigma(v) \quad \text{and} \quad \sum_{u < v} \sigma(u) \sigma(v) = \frac{1}{2} \left[\sum_{u \in \mathcal{V}_n} \sigma(u) \right]^2 - \frac{1}{2} V_n.$$

The second term on the right-hand side of the last equation does not depend on σ . Hence, we conclude that finding the maximizers of p_G is equivalent to finding the maximizers of

$$\frac{1}{2} \log \left(\frac{b_n(1-a_n)}{a_n(1-b_n)} \right) \left[- \frac{1}{2} \sum_{u \sim v} \sigma(u) \sigma(v) + \frac{\rho_n}{2} \left[\sum_{u \in \mathcal{V}_n} \sigma(u) \right]^2 \right].$$

Moreover, the maximizers of the latter expression are the minimizers of

$$- \frac{1}{2} \sum_{u \sim v} \sigma(u) \sigma(v) + \frac{\rho_n}{2} \left[\sum_{u \in \mathcal{V}_n} \sigma(u) \right]^2$$

because $a > b > 0$ implies that $b_n(1-a_n) < a_n(1-b_n)$. □

The following lemma proves (17c).

Lemma 7. *If $\gamma_n/\sqrt{n} \rightarrow 0$ as $n \rightarrow \infty$, then $\gamma_n [\mathbf{z}_n(0) - \mathbf{z}_\infty(0)] \Rightarrow 0$ as $n \rightarrow \infty$.*

Proof. The construction in Algorithm 1 implies that

$$\mathbf{z}_n^k(0) = \frac{1}{V_n^k} \sum_{u \in \mathcal{V}_n^k} I_n^k(u),$$

where the random variables $I_n^k(u)$ are mutually independent and such that

$$P(I_n^k(u) = 1) = \eta \mathbb{1}_{\{k=1\}} + \frac{1-\eta}{2} \quad \text{and} \quad P(I_n^k(u) = -1) = \eta \mathbb{1}_{\{k=2\}} + \frac{1-\eta}{2}.$$

By the central limit theorem, $\sqrt{n} [\mathbf{z}_n(0) - \mathbf{z}_\infty(0)]$ converges weakly to a bivariate normal distribution as $n \rightarrow \infty$. As a result, we conclude that $\gamma_n [\mathbf{z}_n(0) - \mathbf{z}_\infty(0)] \Rightarrow 0$. □

Next we provide the proof of Lemma 2.

Proof of Lemma 2. Let $S_{\mathbb{R}^2}[0, T]$ be the space of càdlàg functions from $[0, T]$ into \mathbb{R}^2 with the Skorohod- J_1 topology. The first two limits in (17) hold with respect to the topology

of uniform convergence over compact sets and thus also with respect to the Skorohod- J_1 topology. Because $S_{\mathbb{R}^2}[0, T]$ is separable, the product $S_{\mathbb{R}^2}[0, T] \times S_{\mathbb{R}^2}[0, T] \times \mathbb{R}^2 \times \mathbb{R}^2$ is separable with respect to the product topology. Therefore, the process

$$\left(\mathbf{z}_m, \gamma_m \left(\frac{\mathcal{M}_m^1}{V_m^1}, \frac{\mathcal{M}_m^2}{V_m^2} \right), \gamma_m [\mathbf{z}_m(0) - \mathbf{z}_\infty(0)], \gamma_m \left(\max_{\sigma \in \Sigma_m(\theta, \theta)} \mathcal{E}^1(\sigma), \max_{\sigma \in \Sigma_m(\theta, \theta)} \mathcal{E}^2(\sigma) \right) \right)$$

is measurable with respect to the Borel σ -algebra associated with the product topology; see [9, Appendix M10]. It follows from [9, Theorem 3.1] that the above process converges weakly to $(\mathbf{z}, 0, 0, 0)$ as $m \rightarrow \infty$ because the right-hand sides of the last three limits in (17) are deterministic processes; see [23, Lemma 9] for further details.

It follows from Skorohod's representation theorem that (18) holds but considering the Skorohod- J_1 topology for the first two limits, instead of the topology of uniform convergence over compact sets. However, the limiting processes in (18a) and (18b) are almost surely continuous, so the limits hold with respect to the latter topology as well. \square

References

- [1] E. Abbe, "Community detection and stochastic block models: Recent developments," *Journal of Machine Learning Research*, vol. 18, no. 177, pp. 1–86, 2018.
- [2] E. Abbe, A. S. Bandeira, and G. Hall, "Exact recovery in the stochastic block model," *IEEE Transactions on Information Theory*, vol. 62, no. 1, pp. 471–487, 2015.
- [3] K. Avrachenkov and M. Dreveton, *Statistical Analysis of Networks*. Now Publishers, 2022.
- [4] —, "Almost exact recovery in noisy semi-supervised learning," *Probability in the Engineering and Informational Sciences*, pp. 1–22, 2024.
- [5] K. Avrachenkov, A. Mishenin, P. Gonçalves, and M. Sokol, "Generalized optimization framework for graph-based semi-supervised learning," in *Proceedings of the 2012 SIAM International Conference on Data Mining*. SIAM, 2012, pp. 966–974.
- [6] A. Barbour, "Density-dependent Markov population processes," *Advances in Applied Probability*, vol. 12, no. 3, pp. 547–548, 1980.
- [7] P. Bedi and C. Sharma, "Community detection in social networks," *Wiley interdisciplinary reviews: Data mining and knowledge discovery*, vol. 6, no. 3, pp. 115–135, 2016.
- [8] S. S. Bhowmick and B. S. Seah, "Clustering and summarizing protein-protein interaction networks: A survey," *IEEE Transactions on Knowledge and Data Engineering*, vol. 28, no. 3, pp. 638–658, 2015.

- [9] P. Billingsley, *Convergence of Probability Measures*, 2nd ed. John Wiley & Sons, 1999.
- [10] C. Bordenave, M. Lelarge, and L. Massoulié, “Nonbacktracking spectrum of random graphs: Community detection and nonregular ramanujan graphs,” *The Annals of Probability*, vol. 46, pp. 1–71, 2018.
- [11] S. Brohee and J. Van Helden, “Evaluation of clustering algorithms for protein-protein interaction networks,” *BMC Bioinformatics*, vol. 7, pp. 1–19, 2006.
- [12] J. Calder, B. Cook, M. Thorpe, and D. Slepcev, “Poisson Learning: Graph based semi-supervised learning at very low label rates,” in *International Conference on Machine Learning*. PMLR, 2020, pp. 1306–1316.
- [13] O. Chapelle, B. Schölkopf, and A. Zien, *Semi-Supervised Learning*. MIT Press, 2006.
- [14] P. Chen and S. Redner, “Community structure of the physical review citation network,” *Journal of Informetrics*, vol. 4, no. 3, pp. 278–290, 2010.
- [15] E. Cruciani, E. Natale, and G. Scornavacca, “Distributed community detection via metastability of the 2-choices dynamics,” in *Proceedings of the AAAI Conference on Artificial Intelligence*, vol. 33, no. 01, 2019, pp. 6046–6053.
- [16] A. Dembo and A. Montanari, “Ising models on locally tree-like graphs,” *The Annals of Applied Probability*, vol. 20, pp. 565–592, 2010.
- [17] S. Dommers, “Metastability of the Ising model on random regular graphs at zero temperature,” *Probability Theory and Related Fields*, vol. 167, pp. 305–324, 2017.
- [18] S. Dommers, F. den Hollander, O. Jovanovski, and F. R. Nardi, “Metastability for Glauber dynamics on random graphs,” *The Annals of Applied Probability*, vol. 27, pp. 2130–2158, 2017.
- [19] S. Dommers, C. Giardinà, and R. van der Hofstad, “Ising models on power-law random graphs,” *Journal of Statistical Physics*, vol. 141, pp. 638–660, 2010.
- [20] S. Fortunato, “Community detection in graphs,” *Physics Reports*, vol. 486, no. 3-5, pp. 75–174, 2010.
- [21] S. E. Garza and S. E. Schaeffer, “Community detection with the label propagation algorithm: A survey,” *Physica A: Statistical Mechanics and its Applications*, vol. 534, p. 122058, 2019.
- [22] M. Girvan and M. E. Newman, “Community structure in social and biological networks,” *Proceedings of the National Academy of Sciences*, vol. 99, no. 12, pp. 7821–7826, 2002.

- [23] D. Goldszajn, S. C. Borst, and J. S. van Leeuwen, “Fluid limits for interacting queues in sparse dynamic graphs,” *arXiv preprint arXiv:2305.13054*, 2024.
- [24] S. Harenberg, G. Bello, L. Gjeltrema, S. Ranshous, J. Harlalka, R. Seay, K. Padmanabhan, and N. Samatova, “Community detection in large-scale networks: a survey and empirical evaluation,” *Wiley Interdisciplinary Reviews: Computational Statistics*, vol. 6, no. 6, pp. 426–439, 2014.
- [25] F. d. Hollander and O. Jovanovski, “Glauber dynamics on the Erdős-Rényi random graph,” *arXiv preprint arXiv:1912.10591*, 2019.
- [26] S. Janson, T. Luczak, and A. Rucinski, *Random Graphs*. John Wiley & Sons, 2011.
- [27] O. Kallenberg, *Foundations of Modern Probability*, 3rd ed. Springer, 2021.
- [28] K. Kothapalli, S. V. Pemmaraju, and V. Sardeshmukh, “On the analysis of a label propagation algorithm for community detection,” in *International Conference on Distributed Computing and Networking*. Springer, 2013, pp. 255–269.
- [29] T. G. Kurtz, “Solutions of ordinary differential equations as limits of pure jump Markov processes,” *Journal of Applied Probability*, vol. 7, no. 1, pp. 49–58, 1970.
- [30] —, “Limit theorems for sequences of jump Markov processes approximating ordinary differential processes,” *Journal of Applied Probability*, vol. 8, no. 2, pp. 344–356, 1971.
- [31] —, “Strong approximation theorems for density dependent Markov chains,” *Stochastic Processes and their Applications*, vol. 6, no. 3, pp. 223–240, 1978.
- [32] K. Liu, S. Mohanty, P. Raghavendra, A. Rajaraman, and D. X. Wu, “Locally stationary distributions: A framework for analyzing slow-mixing Markov chains,” in *2024 IEEE 65th Annual Symposium on Foundations of Computer Science (FOCS)*. IEEE, 2024, pp. 203–215.
- [33] E. Lubetzky and A. Sly, “Universality of cutoff for the Ising model,” *The Annals of Probability*, vol. 45, pp. 3664–3696, 2017.
- [34] F. Menczer, S. Fortunato, and C. A. Davis, *A First Course in Network Science*. Cambridge University Press, 2020.
- [35] E. Mossel, J. Neeman, and A. Sly, “Reconstruction and estimation in the planted partition model,” *Probability Theory and Related Fields*, vol. 162, pp. 431–461, 2015.
- [36] E. Mossel and A. Sly, “Exact thresholds for Ising–Gibbs samplers on general graphs,” *The Annals of Probability*, vol. 41, pp. 294–328, 2013.
- [37] M. Newman, *Networks*. Oxford University Press, 2018.

- [38] M. E. Newman, “Modularity and community structure in networks,” *Proceedings of the National Academy of Sciences*, vol. 103, no. 23, pp. 8577–8582, 2006.
- [39] U. N. Raghavan, R. Albert, and S. Kumara, “Near linear time algorithm to detect community structures in large-scale networks,” *Physical Review E*, vol. 76, no. 3, p. 036106, 2007.
- [40] J. Reichardt and S. Bornholdt, “Statistical mechanics of community detection,” *Physical Review E*, vol. 74, no. 1, p. 016110, 2006.
- [41] H. Saad and A. Nosratinia, “Community detection with side information: Exact recovery under the stochastic block model,” *IEEE Journal of Selected Topics in Signal Processing*, vol. 12, no. 5, pp. 944–958, 2018.
- [42] S. E. Schaeffer, “Graph clustering,” *Computer Science Review*, vol. 1, no. 1, pp. 27–64, 2007.
- [43] J. Shi and J. Malik, “Normalized cuts and image segmentation,” *IEEE Transactions on Pattern Analysis and Machine Intelligence*, vol. 22, no. 8, pp. 888–905, 2000.
- [44] Z. Song, X. Yang, Z. Xu, and I. King, “Graph-based semi-supervised learning: A comprehensive review,” *IEEE Transactions on Neural Networks and Learning Systems*, vol. 34, no. 11, pp. 8174–8194, 2022.
- [45] L. Šubelj, N. J. Van Eck, and L. Waltman, “Clustering scientific publications based on citation relations: A systematic comparison of different methods,” *PloS one*, vol. 11, no. 4, p. e0154404, 2016.
- [46] D. A. Tolliver and G. L. Miller, “Graph partitioning by spectral rounding: Applications in image segmentation and clustering,” in *2006 IEEE Computer Society Conference on Computer Vision and Pattern Recognition (CVPR’06)*, vol. 1. IEEE, 2006, pp. 1053–1060.
- [47] J. E. Van Engelen and H. H. Hoos, “A survey on semi-supervised learning,” *Machine Learning*, vol. 109, no. 2, pp. 373–440, 2020.
- [48] S. Wasserman and K. Faust, *Social Network Analysis: Methods and Applications*. Cambridge University Press, 1994.
- [49] Y. Xing and K. H. Johansson, “Almost exact recovery in gossip opinion dynamics over stochastic block models,” in *2023 62nd IEEE Conference on Decision and Control (CDC)*, 2023, pp. 2421–2426.
- [50] D. Zhou, O. Bousquet, T. Lal, J. Weston, and B. Schölkopf, “Learning with local and global consistency,” *Advances in neural information processing systems*, vol. 16, 2003.

- [51] X. Zhu, Z. Ghahramani, and J. D. Lafferty, “Semi-supervised learning using Gaussian fields and harmonic functions,” in *Proceedings of the 20th International Conference on Machine Learning (ICML-03)*, 2003, pp. 912–919.